AN ABSTRACT OF THE THESIS OF

Hesam E. Shoori J. for the degree of Master of Science in Mechanical Engineering presented on July 15, 2014.

Title: An Approach To Reduced-Order Modeling and Feedback Control For Wave Energy Converters

Abstract approved: _____

Belinda A. Batten

Wave energy holds great promise to be part of the alternative energy portfolio that will provide independence from fossil fuels. As wave energy converter (WEC) technologies mature, designing effective control strategies to extract maximum energy, extend device life, coordinate WEC operation within an array, or mitigate negative impacts of a WEC becomes an increasingly important area of research. However, developing tractable models for the real-time computation of WEC control signals is challenging. This thesis is concerned with developing a model reduction approach for control design that is suitable for application to high fidelity computational fluid-structure interaction. There are many approaches to model reduction; in the last two decades, much attention has been focused on the proper orthogonal decomposition and other singular value decom-

position (SVD) type methods. In the control literature, the balanced truncation is an established approach to model reduction. Balanced POD is a computational approach related to the proper orthogonal decomposition in order to compute balanced truncation of a control system. The work presented in this thesis is the investigation into the applicability of a recently developed model reduction technique, Balanced POD, applied to a WEC fluid-structure interaction problem. We first model a one-dimensional fluid-structure interaction model arising in WEC dynamics heuristically, then design two control strategies for the tracking control of the WEC. Finally, we address the problem of estimating the type of information that can be available to the WEC controller and developing estimates of wave heights and forces that are suitable for control design. The work presented here paves the way for further research regarding the suitability of model reduction techniques applied to WEC problem. The simulation results clearly demonstrate that the reduced order models can successfully capture the fundamental nature of WEC dynamics and can be readily used for control design.

An Approach To Reduced-Order Modeling and Feedback Control For Wave Energy Converters

by

Hesam E. Shoori J.

A THESIS

submitted to

Oregon State University

in partial fulfillment of
the requirements for the
degree of

Master of Science

Presented July 15, 2014
Commencement June 2015

Master of Science thesis of Hesam E. Shoori J. presented on July 15, 2014.

APPROVED:

Major Professor, representing Mechanical Engineering

Head of the School of Mechanical, Industrial, and Manufacturing Engineering

---

Dean of the Graduate School

I understand that my thesis will become part of the permanent collection of Oregon State University libraries. My signature below authorizes release of my thesis to any reader upon request.

Hesam E. Shoori J., Author

ACKNOWLEDGEMENTS

I would like to express my sincere gratitude to my graduate advisor, Prof. Belinda Batten, for the continuous support of my Masters study and research, for her patience, motivation, enthusiasm, and immense knowledge and express my appreciation for all the guidance she offered to me and the knowledge she shared with me.

I would like to also acknowledge my co-advisor, Dr. John Singler, for helping me to better understand the concepts of model reduction techniques and leading instructional discussions.

I would particularly like to thank my friend, Blake Boren, for his helpful notes and valuable advice. It's been a pleasure to have the opportunity to work with him.

I also thank my friends (too many to list here but you know who you are!) for providing support and friendship that I needed.

Last but not the least, I would like to thank my family for all of their encouragement and support throughout the years.

This work supported in part by the National Science Foundation under grant DMS-1217122.

TABLE OF CONTENTS

TABLE OF CONTENTS (Continued)

LIST OF FIGURES

LIST OF FIGURES (Continued)

LIST OF TABLES

NOMENCLATURE

m	$\equiv$	density of the mass in cable-mass system
ρ	$\equiv$	density of the cable in cable-mass system
τ	$\equiv$	tension in the cable
γ	$\equiv$	damping coefficient
k_1	$\equiv$	linear spring stiffness constant for cable-mass system
k_3	$\equiv$	nonlinear spring stiffness constant for cable-mass system
m_0	$\equiv$	wave maker mass
k_0	$\equiv$	stiffness constant for wave maker
β^2	$\equiv$	tension in ocean waves
$k_{l,1}$	$\equiv$	linear stiffness constant of WEC
$k_{l,3}$	$\equiv$	nonlinear stiffness constant of WEC
l	$\equiv$	wave tank length
γ_l	$\equiv$	damping coefficient

Chapter 1: Introduction

Harnessing energy from the ocean presents an attractive potential addition to the patchwork of clean energy sources that could provide alternatives to fossil fuels. Recent estimates from the US Department of Energy place marine energy and in river turbines as potentially providing 25% of the US energy needs. Wave energy conversion, one of the three major types of kinetic ocean energy technology, is where wind energy was 30 years ago. That is, the best type of device is yet unknown, and much research is yet to be done to bring the industry to maturity. A critical piece of this research involves controlling wave energy converters (WECs). There are several objectives that have been considered in control design: maximum energy extraction, energy extraction while maximizing WEC life, minimizing stress due to extreme events [1, 2].

A challenge for controlling WECs is developing tractable models that can be used for real-time computation of WEC control signals. The fluid-structure interactions of the WEC in the ocean and the forces on the WEC are far too complex to use a high fidelity model in this context. Therefore, reduced order models are required. This work is concerned with developing a model reduction approach for control design that is suitable for application to the high fidelity computational fluid-structure interaction.

There are many approaches to model reduction; in the last two decades, much

attention has been focused on the proper orthogonal decomposition and other singular value decomposition (SVD) type methods [3, 4]. One strength of SVD type methods is that they can be applied to data from a computational model or experiments, and little knowledge of the simulation code is required. A challenge to SVD methods is that the model is based on a specific data set, and how well it does in representing behavior outside that dataset is largely unknown. This attribute provides an added challenge when using such models for control design; since controls change the behavior of the system, at times in fundamental ways, can the model derived from an SVD type reduction method capture these changes?

In the control literature, the balanced truncation is an established approach to model reduction [5]. The balanced truncation method is based on system concepts that lead to a reduced order model that captures fundamental aspects of the control system. A challenge to this method is that it requires matrix computations that can be unwieldy, and intractable, especially for large matrix systems that would be encountered in the context of the fluid-structure interaction WEC control problem.

The work in this thesis is a hybridization of the two approaches, with a computational approach related to the proper orthogonal decomposition applied to compute balanced truncations of a control system. Balanced POD, as a recently developed model reduction method, has been applied to a number of applications to date [6–8]. However none of the problems have had the system characteristics of a WEC fluid-structure interaction problem. This work is the first in a planned series of work that investigates the suitability of the balanced proper orthogonal decomposition, or Balanced POD, as a model reduction technique for the fluid-

structure interaction models arising in WEC dynamics.

The applicability of Balanced POD algorithm to parabolic systems has been verified and its convergence behavior has been studied in previous works [9]. However, this technique may not show great promise for highly oscillatory systems. Moreover, feasibility of the Balanced POD application to hyperbolic systems, such as those arising in WEC dynamics, is yet to be shown. Therefore, this work first strives to investigate the suitability of the algorithm when applied to a hyperbolic system in order to get a sense that it properly works for WEC fluid-structure interaction problem.

As a first step to apply these methods to this new domain, we take a simplified approach towards the modeling of a WEC interacting with ocean waves. In order to capture the fundamental nature of the WEC problem, a simple one-dimensional fluid-structure interaction problem in a wave tank is considered and synthesized. Specifically, we consider a point absorber buoy that is a WEC which has a float on the surface of the water and is held in place by its connections to the seabed and moves in relation to a spar. Figure 1.1 shows such a point absorber buoy.

In this work, we use a simplified model for a point absorber buoy: a mass that is supported by a spring that is attached to the ocean bottom. The mass represents the motion of the float and the spring represents the buoyancy forces of the waves on the WEC. On either side of the mass, we use a wave equation to simply model the ocean hydrodynamics as illustrated in Figure 1.2.

The mathematical equations for the model considered here are similar to those used for a cable-mass problem, researched extensively by Burns and King [10].

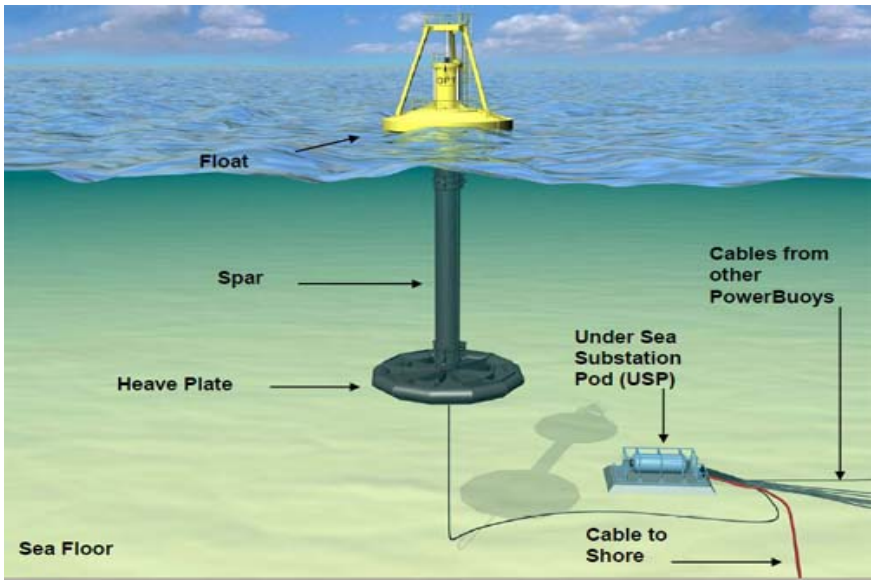

Figure 1.1: A point absorber WEC

Their research can help us to understand the properties of this model. Particularly, the motion of the WEC has the same dynamics as the motion of the mass in the previous literature. Appropriate choices of boundary conditions to be employed to the WEC problem in a wave tank will be discussed later.

It should be noted that we will use "reduce-then-design"approach to obtain a low-order controller for the WEC problem. This approach involves reducing the PDE model using a model reduction technique first and then applying a control strategy to it. Figure 1.3 shows the diagram describing the "reduce-then-design"approach.

Once the reduced order model is obtained, optimal control designs will be applied with the goal of comparing the reduced order control with the control for

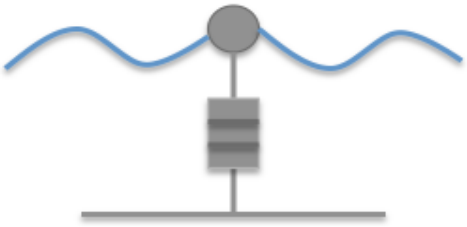

Figure 1.2: A simplified point absorber buoy model

the high fidelity model of this idealized model. In the first step, we will use the standard LQR tracking controller with a periodic desired WEC position to test the basic control design. Then, the control method will be extended to testing an approach to state estimation that can be utilized with the information limits inherent in ocean operations using LQG control.

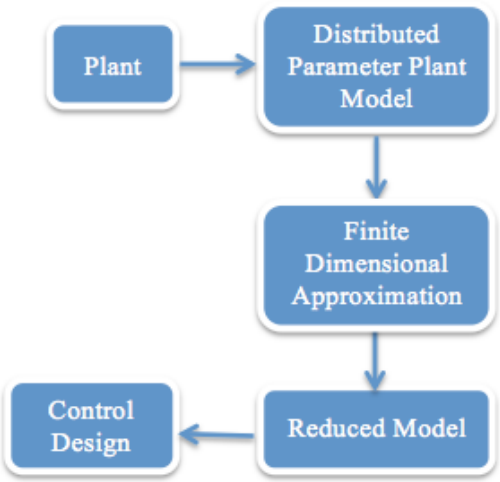

Figure 1.3: "Reduce then Design" diagram

1.1 Contributions

Major contributions of this thesis involve the following items:

1. Verifying the applicability of balanced POD model reduction technique to hyperbolic systems especially when applied to WEC problem;

2. Developing a simplified approach to study the high fidelity fluid-structure interaction problem arising in WEC dynamics;

3. Comparing multiple sensor locations to use in control calculations and developing LQR and LQG tracking systems for two different system configurations;

4. Constructing the desired tracking function for the WEC to follow by wave height estimation using buoy data.

Note that the work done in this thesis is the first in a planned series of work that attempts to investigate the application of model reduction techniques to wave energy research area. A heuristic 1D PDE model for a wave energy converter in a wave tank that is studied in this thesis could serve as a test bed for further research, which can be later extended to multiple spatial dimensions in a real ocean.

Chapter 2: Literature Review

2.1 Wave Energy Overview

The decrease in the natural resources resulting from increasing demand of energy necessitates the utilization of renewable energy sources. The potential for extracting energy from ocean waves as a sustainable energy source is considerable. According to [11], it is estimated that wave energy has potential contribution of 2,000 TWh/year in the world electricity market. However, wave energy converter technology is still far from being competitive compared to other renewable energy sources [12].

The devices that convert the wave energy into electricity are called Wave Energy Converters. In the last decades, there has been extensive research into the development of WECs that can be found in several surveys [13–17]. The earliest recorded interest in utilizing ocean waves for on-shore use is a patent for a wave-energy-conversion device filed by a French inventor in 1799. Since then, there has been a plethora of ideas on how best to convert wave energy. In contrast to the modern wind industry, there is yet no single dominant technological paradigm for ocean-wave-energy conversion. However, past and current designs can be classified within three main categories, namely, oscillating water column (OWC), overtopping, and oscillating body (for more details, see [12]). For example, Figure 2.1

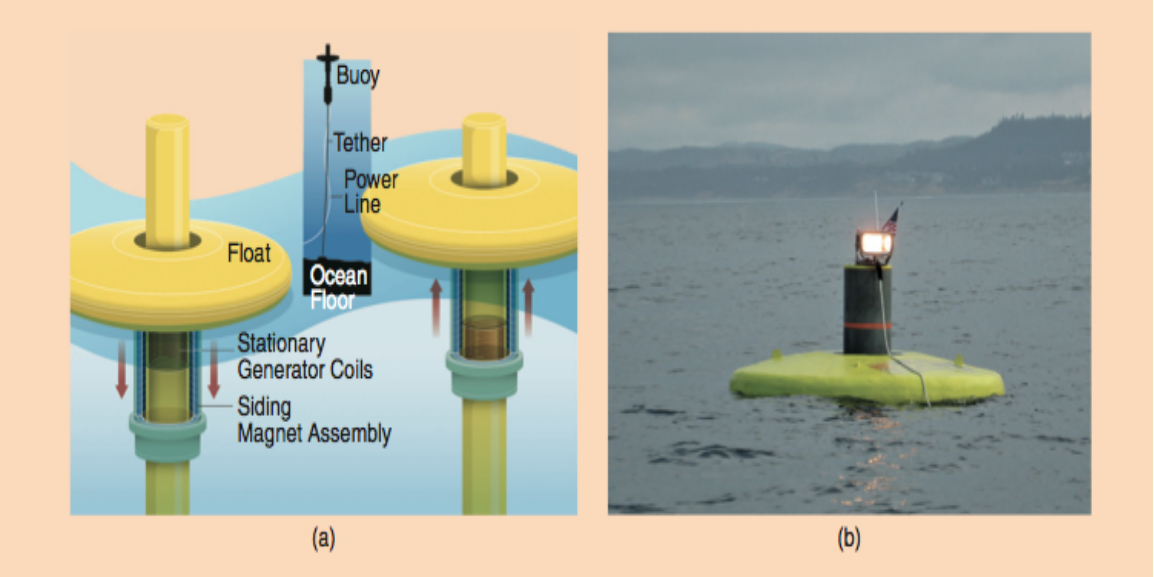

Figure 2.1: The L10 Point Absorber wave energy converter (WEC). (a) shows the operation of the L10 point absorber WEC. (b) shows the L10 deployed at Yaquina Head, Oregon, in September 2008

shows a point absorber WEC which is an example of oscillating body devices that was developed and tested by Columbia Power Technologies, in collaboration with Oregon State University and with funding support from the U.S. Navy and Columbia Power Technologies. This point absorber is called the L10, for "linear 10 kW".

Commercializing this energy source requires systems and control tools to understand the resource and how to efficiently maximize the energy extracted from waves. Control systems can be used for a variety of reasons in the context of wave energy, such as maximizing the energy extraction from waves, minimizing excessive wear or damage to devices from unusually large waves or storm events, and

coordinating arrays of wave energy converters (WECs).

Many areas in wave energy control are ripe for further research. For example, developing control strategies that balance energy conversion with damage mitigation to maximize the overall revenue can be significant. Optimal control approaches with appropriate objective functions have the potential to address this challenge [18]. Moreover, as large waves and devices exhibit significant nonlinear behavior, robust and fast nonlinear control and modeling approaches are needed. Adaptive control approaches, such as maximum power point tracking [19,20], may be a practical and effective approach to dealing with nonlinearities and changing operating conditions. As more sophisticated models of the fluid-structure interactions are coupled to device models to more accurately predict forces, reduced-order model and control designs are important, that will be the main focus of this thesis.

2.2 Model Reduction Techniques

Distributed parameter systems are systems whose state spaces are infinite dimensional. Therefore, they are often called as infinite dimensional systems [21]. Problems that are governed by partial differential equations (PDEs) or delay differential equations are the examples of such systems. A PDE system that is introduced in an infinite dimensional space necessitates the application of a numerical approximation scheme to give the corresponding finite dimensional system for computational purposes. In many cases, when a PDE system is discretized using a numerical approximation method, the number of the resulting system states will be still

very large. In the case that a large approximating system is used in control design, a large-scale controller will result. The real-time control of such systems such as fluid-structure interactions becomes impractical. Since we are interested in design of controllers that can be readily used for real time purposes, large-scale models or controllers should be reduced at some point using model reduction techniques [6], [22–24].

In a model reduction technique, a large, high fidelity model is replaced by a smaller, more computationally tractable model that can closely approximate the original dynamics. In other words, model reduction involves reducing a given dynamic finite element model to one with fewer degrees of freedom while maintaining the dynamic characteristics of the system. For example in [25], Lee and Tran employ two reduced order methods for feedback control of Kuramoto-Sivashinsky equation. Rowley develops a model reduction for fluid flows in [6]. In general, the model reduction technique should have the following properties:

- Applicability to large class of dynamical systems
- Computationally tractable
- Minimizing a reduction error between the full-order and the reduced-order model

A model reduction technique for models of high complexity is needed to:

- Conduct simulations in a short period of time with limited memory storage capacity (need for computational speed)

- Allow for model based control design
- Perform on-line optimization of processes
- Improve numerical accuracy of the model (large-scale systems are likely to be ill-conditioned)
- Allow for the implementation of the model on a chip

Some of the motivating examples requiring the reduction techniques are high frequency VLSI circuits [26], biomedical models [27], aerodynamic aircraft models [28], international space station, diffusion and convection [29], computational fluid dynamics models and fluid-structure interactions and so on. In all these cases, any realistic model will require many state variables to be described accurately. The resulting complexity necessitates the use of a simplification method to perform a simulation in an acceptable amount of time or for the design of a low order controller.

There are many approaches to model reduction; recently there has been much attention on the singular value decomposition (SVD) type methods, a number of which can be found in [3, 30]. One strength of SVD type methods is that they can be applied to data from a computational model or experiments, and little knowledge of the simulation code is required. A challenge to SVD methods is that the model is based on a specific data set, and how well it does in representing behavior outside that dataset is largely unknown. This attribute provides an added challenge when using such models for control design; since controls change the

behavior of the system, at times in fundamental ways, can the model derived from an SVD type reduction method capture these changes? Therefore, a more sophisticated reduction method might be needed for control applications that can capture the general behavior of the system.

2.2.1 Proper Orthogonal Decomposition

Proper orthogonal decomposition (POD), a method used by many researchers in the past 20 years (Lumey [31], Sirovich [32], Aubry et al [33], Holmes et al [34] and others) is considered to be a powerful reduction method that tries to project the high dimensional model into a low dimensional approximate model. More specifically, POD aims at defining the basis functions φ_i to use for Galerkin projection that best capture the important modes for the model dynamics. The POD technique is applied to a set of data called snapshots that are normally obtained from system measurements or numerical solutions at different time steps. POD technique has been widely used in different areas: from modeling fluid flows [35–37] and structural vibrations [38] to image processing and pattern recognition [39].

In the POD algorithm [40], it is assumed that we have a set of data taken form a partial differential equation, $x(s,t)$, representing the function values at location s and time t. Then, as discussed in the previous section, a low-order corresponding system is obtained as

$$x_r(s,t) = \sum_{i=1}^{n} q_i(t)\varphi_i(s) \tag{2.1}$$

where $q_i(t)$ represent the coefficients and $\varphi_i(s)$ are fixed orthonormal basis functions for the lower dimensional subspace, i.e.

$$\langle \varphi, \varphi \rangle = \|\varphi\|^2 = 1. \tag{2.2}$$

The aim of the POD is to find modes $\varphi_i(s)$ that are able to minimize the error between the original data x and the projected data x_r. The coefficients can be computed using orthonormality

$$q_i(t) = \langle x(s,t), \varphi_i(s) \rangle = \int x(s,t)^T \varphi_i(s) ds. \tag{2.3}$$

It can be shown that the POD modes can be computed by solving the eigenvalue problem

$$R\varphi(s) = \lambda\varphi(s) \tag{2.4}$$

in which R is a nonnegative symmetric operator

$$R\varphi(s) = \int T(x,x')\varphi(s) ds' \tag{2.5}$$

$$T(x,x') = \overline{x(s,t)x(s,t)^T} \tag{2.6}$$

where overbar denotes the time average. Lastly, the optimal projection is given by

$$P_r = \sum_{i=1}^{r} \varphi_i(s)\varphi_i(s)^T. \tag{2.7}$$

One of the main properties of POD is that it establishes a projection on the subspace such that the projection will contain the most information for a given number of modes. There are many extensions to this approach such as methods for computing modes from incomplete data [41], traveling POD modes [42], scaling POD modes for self-similar solutions [43–45], and shift modes [46] for better capturing transient behavior.

2.2.2 Balanced Truncation

One major problem with the concept of POD is that POD determines the modes based on the most energetic features, while low-energy features might be important to the systems dynamics. Balanced truncation is an alternative method which is not merely based on energetic significance. Balanced truncation was first introduced by Moore [23]. Balancing provides a system realization of (A^b, B^b, C^b) for a PDE system

$$\dot{x}(t) = Ax(t) + Bu(t) \tag{2.8}$$

$$y(t) = Cx(t), \tag{2.9}$$

in which the controllability and observability gramians are equal and diagonal in the new coordinates.

The underling idea is to consider both the inputs and the outputs of the system when trying to construct the reduced order model by truncating the states that are least controllable and least observable. Let $G(s) = C\left(SI - A\right)^{-1} B$ and $G_r(s) = C_r\left(SI_r - A_r\right)^{-1} B_r$ be the transfer functions of the original and the reduced systems. Then the balanced truncation error holds in the bound

$$\left\|G - G_r\right\|_\infty \leqslant 2 \sum_{k>r} \sigma_k \tag{2.10}$$

where σ_k is the Hankel singular value ordered from the greatest to least and H_∞ norm is the largest singular value of the function along the imaginary axis.

In order to determine to what degree the states are controllable and observable, the controllability and observability gramians are defined based on controllability and observability operators. In the original coordinates, these two matrices might not be equal. So balanced truncation first attempts to find a balancing transformation that can transform these two matrices into a new coordinate in which the controllability and observability gramians are equal and diagonal. Dullerud and Paganini [47], or Datta [48] introduce algorithms for computing balancing transformations. Once the transformed coordinates are computed, the truncation procedure only retains those states that are the most controllable and observable based on the eigenvalues of the product of the controllability and observability gramians, also known as the Hankel singular values.

A challenge to this method is that it requires matrix computations that can be unwieldy, and intractable, especially for large matrix systems that would be encountered in the context of the fluid-structure interaction WEC control problem. Lall et al [49] presents the snapshot-based approach to solve this problem. In addition, an algorithm for computing the balancing transformation directly from snapshots can be found in [50].

2.2.3 Balanced POD

Balanced POD is a recently developed model reduction technique that has received much attention among engineers. Balanced POD is an algorithm that attempts to approximate the well-known balanced truncation reduced order model described in the previous section. Because an approximation to a PDE system can be very large, computing a balanced truncation might become quite complicated. This challenge is addressed in Balanced POD technique. Since this method will serve as our main methodology in this work, we will thoroughly discuss the algorithm in the next chapter.

Chapter 3: Balanced Proper Orthogonal Decomposition: An Example Problem

In this chapter, we provide detailed explanation of balanced POD algorithm as our methodology along with an example problem. We then turn our attention to developing a reduced order model for a conventional cable-mass system via balanced POD method, which further helps us to model and control a point absorber WEC.

3.1 Balanced POD

3.1.1 Balanced POD Overview

Rowley developed Balanced POD for large-scale systems of ordinary differential equations in [6] that is similar to the method of snapshots in POD technique. The algorithm has been widely applied to create accurate reduced order models of many spatially discretized PDE systems. Rowley's Balanced POD method is extended for reduced order model reduction of infinite dimensional systems in [51]. Balanced POD is considered at the PDE level in [52], [9], [7], [8]. Also, the convergence of the algorithm is proven in [9].

Described in [23], balanced truncation provides a reduced order model of the

form

$$\dot{a}(t) = A_r a(t) + B_r u(t) \qquad a(0) = a_0 \tag{3.1}$$

$$y_r(t) = C_r a(t) \tag{3.2}$$

for the infinite dimensional linear system

$$\dot{x}(t) = Ax(t) + Bu(t) \qquad x(0) = x_0 \tag{3.3}$$

$$y(t) = Cx(t) \tag{3.4}$$

where (A, B, C) are operators acting on the Hilbert space X with inner product $(.,.)$ and corresponding norm $\|.\| = (.,.)^{1/2}$. The linear operator $A : D(A) \subset X \to X$ is assumed to generate an exponentially stable C_0-semigroup e^{At}, and the operators $B : U \to X$ and $C : X \to Y$ are assumed to be bounded. These operators can be rewritten in the form

$$Bu = \sum_{j=1}^{m} b_j u_j \qquad Cx = [(c_1, x), ..., (c_p, x)]^T \tag{3.5}$$

in which the input to the system is an m dimensional vector $u = [u_1, ..., u_m]^T \in U$. This form of representation allows for a computationally simple gramians. We first define the following functions

$$w_j(t) = e^{At} b_j \qquad j = 1, 2, ..., m \tag{3.6}$$

where $w_j(t)$ can intuitively be found by simulating the forward differential equation

$$\dot{w_j}(t) = Aw_j(t) \qquad w_j(0) = b_j. \tag{3.7}$$

This definition helps to rewrite the controllability operator and its adjoint operator as

$$\mathcal{B}u = \int_0^\infty e^{At}Bu(t)dt = \int_0^\infty \sum_{j=1}^{m} w_j(t)u_j(t)dt \tag{3.8}$$

$$[\mathcal{B}^*x](t) = [(w_1(t), x), ..., (w_m, x)]^T. \tag{3.9}$$

Then, the controllability gramian is defined as

$$W_c x = \mathcal{B}\mathcal{B}^* x = \int_0^\infty \sum_{j=1}^{m} w_j(t)(w_j(t), x)dt. \tag{3.10}$$

In order to proceed with the observability gramian, the same procedure as for B is used. Therefore, let us define

$$z_j(t) = e^{A^*t}c_j \qquad \text{for} \quad j = 1, 2, ..., p. \tag{3.11}$$

Just like before, $z_j(t)$ is the solution to the following forward differential equation

$$\dot{z_j}(t) = A^* z_j(t) \qquad z_j(0) = c_j \tag{3.12}$$

which helps to redefine the observability operator and its joint operator

$$[\mathcal{C}x](t) = [(z_1(t), x), ..., (z_p, x)]^T \tag{3.13}$$

$$\mathcal{C}^* y = \int_0^\infty e^{A^* t} C^* y(t) dt = \int_0^\infty \sum_{j=1}^{p} z_j(t) y_j(t) dt. \tag{3.14}$$

Therefore, the observability gramian can be rewritten as

$$W_o x = \mathcal{C}^* \mathcal{C} = \int_0^\infty \sum_{j=1}^{p} z_j(t)(z_j(t), x) dt. \tag{3.15}$$

The forward differential equations defined above (3.7), (3.12) are used to obtain approximations $x^n(t)$ and $z^n(t)$ of the solutions $x(t)$ and $z(t)$. These equations should be simulated in time until the approximate solutions are nearly zero. The Hankel operator defined before is then given by

$$[Hu](t) = [\mathcal{C}\mathcal{B}](t) = \int_0^\infty C e^{A(t+s)} B u(s) dt = \int_0^\infty \sum_{j=1}^{m} (z_j(t), w_j(t)) dt. \tag{3.16}$$

In order to compute the gramians, we can use the quadrature approach to approximate the time integrals

$$w_c x = \int_0^\infty \sum_{j=1}^{m} w_j(t)(w_j(t), x) dt \quad \approx \quad \tilde{w}_c^{n_1} x = \sum_{i=1}^{m} \sum_{j=1}^{n_1} \alpha_j^2 w_i(t_j)(w_i(t_j), x) \tag{3.17}$$

$$w_o x = \int_0^\infty \sum_{j=1}^{m} z_j(t)(z_j(t), x) dt \quad \approx \quad \tilde{w}_o^{n_2} x = \sum_{i=1}^{p} \sum_{k=1}^{n_2} \beta_k^2 z_i(t_k)(z_i(t_k), x) \tag{3.18}$$

in which $\{t_j, t_k\}$ and $\{\alpha_j^2, \beta_k^2\}$ are quadrature points and weights, respectively.

These so-called empirical gramians can be arranged into vector forms of dimensions mn_1 and pn_2.

$$\tilde{w} = [\alpha_1 w_1(t_1), ..., \alpha_{n1} w_1(t_{n1}), ..., \alpha_1 w_m(t_1), ..., \alpha_{n1} w_m(t_{n1})]^T \tag{3.19}$$

$$\tilde{z} = [\beta_1 z_1(t_1), ..., \beta_{n2} z_1(t_{n2}), ..., \beta_1 z_p(t_1), ..., \beta_{n2} z_p(t_{n2})]^T. \tag{3.20}$$

It can be shown that the product of the gramians can be represented by matrix Γ using the empirical grammians [53]

$$\Gamma_{ij} = (\tilde{z}_i, \tilde{w}_j). \tag{3.21}$$

We know that the eigenvalues of the product of the gramians are used to construct the reduced order model. Therefore, the singular value decomposition of Γ gives us the approximate singular values

$$\Gamma = U\Sigma V^* = \begin{bmatrix} U_1 & U_2 \end{bmatrix} \begin{bmatrix} \Sigma_1 & 0 \\ 0 & 0 \end{bmatrix} \begin{bmatrix} V_1^* \\ V_2^* \end{bmatrix} = U_1 \Sigma_1 V_1^*, \tag{3.22}$$

where Σ_1 is diagonal and is defined in $R^{s \times s}$ in which $s = rank(\Gamma)$. Using the above SVD, we approximate the Balanced POD modes and the adjoint ones by

$$[\varphi_1, ..., \varphi_s]^T = \Sigma_1^{-1/2} V_1^* \tilde{w} \tag{3.23}$$

$$[\psi_1, ..., \psi_s]^T = \Sigma_1^{-1/2} U_1^* \tilde{z}. \tag{3.24}$$

In order to get the reduced order system, we have to pick $r < s = rank(\Gamma)$ so that we only need the first r balanced POD modes to be computed

$$[\varphi_1, ..., \varphi_r]^T = \Sigma_r^{-1/2} V_r^* \tilde{w} \tag{3.25}$$

$$[\psi_1, ..., \psi_r]^T = \Sigma_r^{-1/2} U_r^* \tilde{z} \tag{3.26}$$

in which Σ_r, U_r and V_r are truncated matrices of Σ_1, U_1 and V_1. Finally, we form the matrices in the reduced order model using truncated balanced POD modes

$$A_r = [(A\varphi_j, \psi_i)] \in R^{r\times r} \qquad B_r = [(b_j, \psi_i)] \in R^{r\times m} \tag{3.27}$$

$$C_r = [(\varphi_j, c_i)] \in R^{p\times r} \qquad a_0 = [(x_0, \psi_1), ..., (x_0, \psi_r)]^T \in R^r. \tag{3.28}$$

The Balanced POD algorithm can be summarized in three steps as:

1. Obtain approximations $w^n(t)$ and $z^n(t)$ of the solutions $w(t)$ and $z(t)$ of the forward and adjoint differential equations (3.7), (3.12).

2. Use the approximate simulation data $\{z_i^N(t)\}$ and $\{w_j^N(t)\}$ to compute Balanced POD singular values $\{\sigma_k\}$ and modes $\{\varphi_k, \psi_k\}$.

3. Choose r and form the approximate balanced reduced order model using (3.27)

3.1.2 Example of Balanced POD applied to a PDE system

In order to assess the performance of the Balanced POD algorithm described above when applied to a model problem, we consider a very simple 1D heat equation with Dirichlet boundary condition on the left and Neumann boundary control on the right

$$w_t(t,x) = \mu w_{xx}(t,x) \tag{3.29}$$

$$w(t,0) = 0, \qquad w_x(t,1) = u(t) \tag{3.30}$$

with point observation defined as

$$y(t) = w(t,x_0) \tag{3.31}$$

where $0 < x_0 \leq 1$.

We apply standard finite element method to get an approximation to this system. Using the variational form of the problem, we multiply by a test function ϕ that is defined in the Hilbert space

$$V = \{\phi \in H^1(0,1) : \phi(0) = 0\}. \tag{3.32}$$

Integrating by parts yields the weak form of the system

$$\int_0^1 w_t(t,x)\phi(x)dx + \mu \int_0^1 w_x(t,x)\phi_x(x)dx = \mu u(t)\phi(1). \tag{3.33}$$

Note that the input operator is defined by

$$\langle Bu, \phi \rangle = \phi(1)u, \tag{3.34}$$

which indicates that B equals δ_1, the Dirac delta function at $x = 1$. Also, the output operator is defined by $C\phi = \phi(x_0)$, i.e., $C = \delta_{x0}$. For the spatial discretization, we use standard piecewise linear finite elements (linear B-splines) with equally spaced nodes for the total length of 1m. We choose a basis $\{e_i\}_{i=1}^{N}$ for the approximating space. Therefore, the state is approximated as

$$w(t, x) \approx w^N(t, x) = \sum_{i=1}^{N} q_i(t) b_i(x) \tag{3.35}$$

where $b_i(x)$ denotes the linear splines. Substituting this approximation of the state into the weak form (3.33) yields the finite dimensional system

$$M \frac{d}{dt} q(t) + Aq(t) = B_0 u(t) \tag{3.36}$$

in which

$$M_{ij} = \int_0^1 b_i(x) b_j(x) dx \tag{3.37}$$

$$A_{ij} = \mu \int_0^1 b_i'(x) b_j'(x) dx \tag{3.38}$$

$$B_0 = \mu [b_1(1), b_2(1), ..., b_N(1)]^T. \tag{3.39}$$

We now apply the Balanced POD algorithm to this system to get a reduced order

approximation. Here, we set $x_0 = 0.5$ and choose the number of finite element nodes large enough so that the error is converged. Table 3.1 shows the Balanced POD error for various values of r, order of the reduction. Figure 3.1 shows the approximate Hankel singular values computed which shows the rapid convergence of the Hankel singular values with mesh refinement.

Table 3.1: Balanced POD error for various r values

system	r = 3	r = 4	r = 5
BPOD error	8.8×10^{-3}	1.7×10^{-3}	2.6×10^{-4}

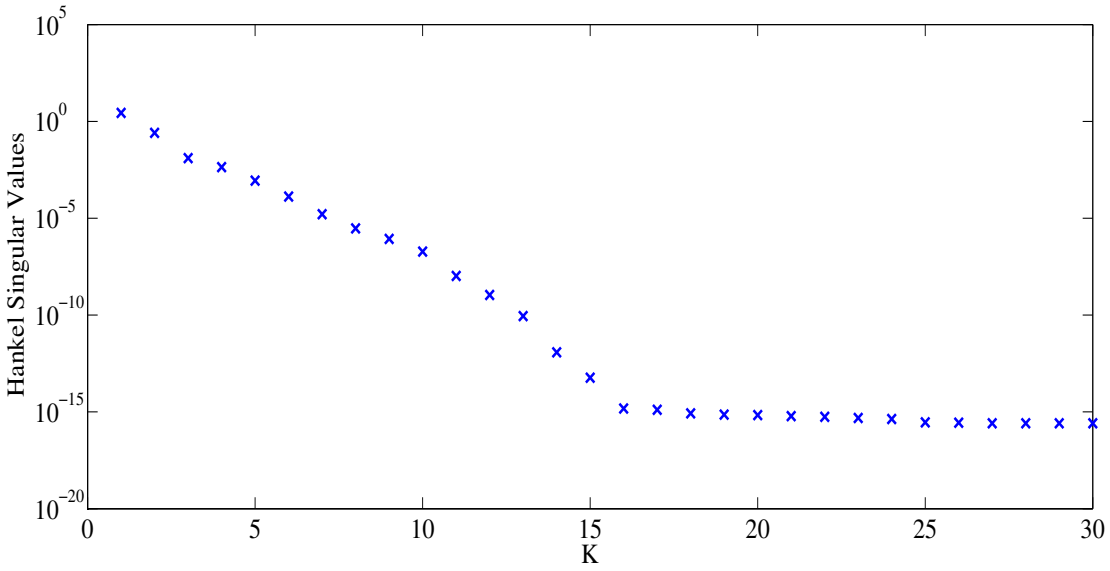

Figure 3.1: Approximate Hankel Singular Values

3.2 Reduced Order Model for a Conventional Cable-Mass System

Before we turn our attention into the design of a low order system for a wave energy converter which will be represented by a 1D PDE model, the conventional cable-mass system described in (Nayfeh, et. Al., 1992) is addressed in this section. The purpose of this study is to gain insight into the application of model reduction techniques for wave equations and also to ensure that Balanced POD algorithm has the potential to work when applied to a hyperbolic system, especially, wave problems in multiple space dimensions with nonlinear behavior as observed in cable-mass model. Balanced POD has almost exclusively been applied to parabolic problems. To the best of author's knowledge, Balanced POD has only been applied once to a second-order vibrations problem [7]. So, this section aims at using Balanced POD on a wave problem to get a sense that it really does work for these problems.

The cable-mass system studied in [10], is considered to be a hybrid distributed parameter system. This model consists of an elastic cable that is fixed at one end and attached to a mass at the other, with a nonlinear spring supporting the mass. The motion of the elastic cable is governed by the wave equation subject to appropriate boundary conditions. Figure 3.2 shows the cable-mass system.

The equations governing the system are

$$\rho\frac{\partial^2}{\partial t^2}w(t,s) = \frac{\partial}{\partial s}[\tau\frac{\partial}{\partial s}w(t,s) + \gamma\frac{\partial^2}{\partial t\partial s}w(t,s)], \quad 0 < s < l, \quad t > 0 \tag{3.40}$$

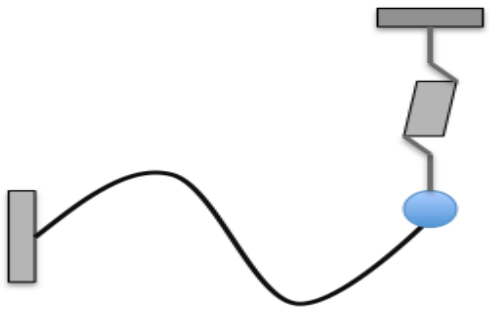

Figure 3.2: Cable-mass system

$$m\frac{\partial^2}{\partial t^2}w(t,l) = -[\tau\frac{\partial}{\partial s}w(t,s) + \gamma\frac{\partial^2}{\partial t\partial s}w(t,s)] - k_1 w(t,l) - k_3[w(t,l)]^3 + u(t) \tag{3.41}$$

with boundary condition

$$w(t,0) = 0 \tag{3.42}$$

and initial conditions

$$w(0,s) = w_0(s) \quad \frac{\partial}{\partial t}w(0,s) = w_1(s) \tag{3.43}$$

where $w(t,s)$ indicates the displacement of the elastic cable at time t and position s, $w(t,l)$ represents the position of the mass at time t, m is the mass of the cable, ρ is the density, τ represents the tension in the cable and γ is a damping coefficient. k_1 and k_3 are spring constants with the latter describing the nonlinear effects of the spring. We also assume that there are two observations available as the sensed

information, which are the position and the velocity of the mass defined by

$$y_1(t) = w(t,l) \quad y_2(t) = \frac{\partial}{\partial t} w(t,l). \tag{3.44}$$

This cable-mass problem can be intuitively used as a simplified approach to capture the fundamental nature of the WEC problem in a one-dimensional (in space) fluid-structure interaction problem in a wave tank. Particularly, the mass in the cable-mass system models a point absorber buoy that is supported by a spring that is attached to the ocean bottom. The wave equation similarly represents the incident ocean waves reaching the WEC. We will discuss more in the next chapter.

3.2.1 Finite Approximations

In order to obtain a finite dimensional system (lumped system) suitable for computation, we will apply a finite element approximation method to the above system as can be found in [10]. First of all, we need to establish the variational form (weak form) of the problem. Multiplying the equations (3.40), (3.41) by a test function $\phi(s)$ and integrating by parts twice yields the weak form

$$\begin{aligned} \int_0^l \rho \frac{\partial}{\partial t} v(t,s)\varphi_1(s)ds + \int_0^l [\tau \frac{\partial}{\partial s} w(t,s) + \gamma \frac{\partial}{\partial s} v(t,s)] \frac{d}{ds}\varphi_1(s)ds \\ + m\frac{\partial}{\partial t} v_l \varphi_1(l) + [k_1 w_l + k_3 w_l^3]\varphi_1(l) = u(t)\varphi_1(l) \end{aligned} \tag{3.45}$$

where $\varphi(s)$ is defined in the Hilbert Space V

$$V = \phi \in H^1(0,1) : \phi(0) = 0. \tag{3.46}$$

Now, a finite element approximation scheme can be applied to the variational form to yield a finite dimensional system. Using linear splines to approximate the position of the cable, the system states are computed as

$$\begin{bmatrix} w(t,s) \\ w(t,l) \end{bmatrix} \approx \begin{bmatrix} w^N(t,s) \\ w^N(t,l) \end{bmatrix} = \sum_{i=1}^{N} \zeta_i^N(t) e_i^N(s) = \begin{bmatrix} \sum_{i=1}^{N} \zeta_i^N(t) b_i^N(s) \\ \zeta_N^N(t) \end{bmatrix} \tag{3.47}$$

where N denotes the number of splines in the interval $[0,l]$, $\{b_i^N(s)\}_{i=1}^{i=N}$ is the linear B-splines. The first order finite dimensional system is obtained by substituting the approximation into the weak form in (3.45)

$$\frac{d}{dt}x^N(t) = A^N x^N(t) + F^N(x^N(t)) + B^N u(t) \tag{3.48}$$

$$x^N(0) = x_0^N \tag{3.49}$$

$$y^N(t) = C^N x^N(t) \tag{3.50}$$

where $x^N(t) = [\zeta^N(t), \frac{d}{dt}\zeta^N(t)]^T, x_0^N = [\zeta_0^N, \zeta_1^N]^T$ and

$$A^N = \begin{bmatrix} 0 & I \\ -M^{-N}A_0^N & -M^{-N}D_0^N \end{bmatrix} \quad B^N = \begin{bmatrix} 0 \\ M^{-N}B_0^N \end{bmatrix} \tag{3.51}$$

$$F^N(x^N(t)) = \begin{bmatrix} 0 \\ -M^{-N}F_0^N(w^N(t)) \end{bmatrix}, \quad C^N = \begin{bmatrix} 0_{1\times N-1} & 1 & 0_{1\times N-1} & 0 \\ 0_{1\times N-1} & 0 & 0_{1\times N-1} & 1 \end{bmatrix} \tag{3.52}$$

in which

$$[M^N]_{ij} = \int_0^l \rho b_i^N(s) b_j^N(s) ds + m b_i^N(l) b_j^N(l), \quad i,j = 1,...,N \tag{3.53}$$

$$[D_0^N]_{ij} = \int_0^l \gamma \frac{d}{ds} b_i^N(s) \frac{d}{ds} b_j^N(s) ds, \quad i,j = 1,...,N \tag{3.54}$$

$$[A_0^N]_{ij} = \int_0^l \tau \frac{d}{ds} b_i^N(s) b_j^N(s) ds + k_1 b_i^N(l) b_j^N(l), \quad i,j = 1,...,N \tag{3.55}$$

$$F_0^N(\zeta^N) = k_3 [w_N^N]^3 \tag{3.56}$$

$$B_0^N = [b_1^N(l), b_2^N(l), ..., b_N^N(l)]^T. \tag{3.57}$$

The uncontrolled simulation of the cable-mass system for the mass position and the midcable position can be found in [24].

3.2.2 Applying Balanced POD

In the previous section, we derived a finite element approximation of the system. In this section, we apply Balanced POD to the model developed above to see how it performs.

Recall that the first step to compute the Balanced POD is to solve two linear ODEs using the system matrices A, B and C. In order to have convergent solutions

$(w(t), z(t))$ for the two sets of forward ODEs, we picked initial time value to be 30 seconds so as to allow for stable reduced order systems irrespective of the order of balanced realization (r). Then, approximate Hankel singular values were computed using various number of basis functions. Figure 3.3 illustrates these values for three different numbers of basis function $(N = 16, 32, 64)$. Figure 3.3

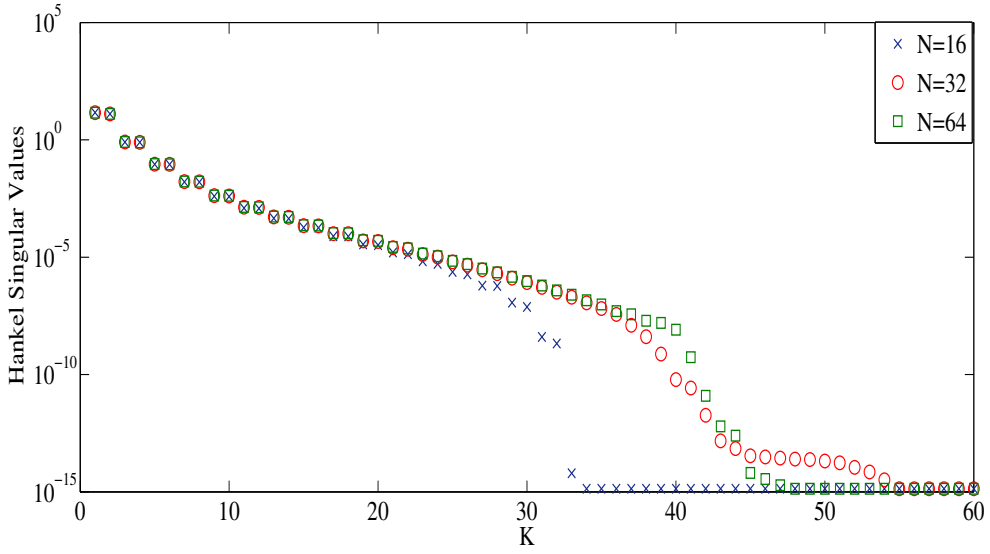

Figure 3.3: Approximate Hankel Singular Values

shows the rapid convergence of the Hankel singular values with mesh refinement. Based on the convergence shown in the plot above, the approximating system arising from $N = 32$ basis functions (and 64 states) was chosen as the "high order system". To determine the size of reduced order system that would further be used for the control computations, we computed the error in system approximation for various values of r. Those are shown for the cable-mass system in Table 3.2 below.

Table 3.2: Balanced POD error for various r values

system	r = 4	r = 6	r = 8
BPOD error	0.4323	0.0787	0.0191

Taking the reduced order model corresponding to order 6 ($r = 6$), the input-output response of the cable-mass PDE and the reduced order model are compared to show the performance of the reduction method using uncontrolled (open-loop) simulations. In this simulation, the input function is chosen to be $u(t) = \sin(t)$. Figure 3.4 depicts the displacement of the mass (or the WEC) for uncontrolled simulation under this chosen input. We note that the reduced order model can approximate quite well the high order system in the open-loop simulation. This assures us the Balanced POD algorithm has the potential to work for hyperbolic systems, which later helps us to obtain a reduced order model for a wave energy converter in fluid-structure interaction.

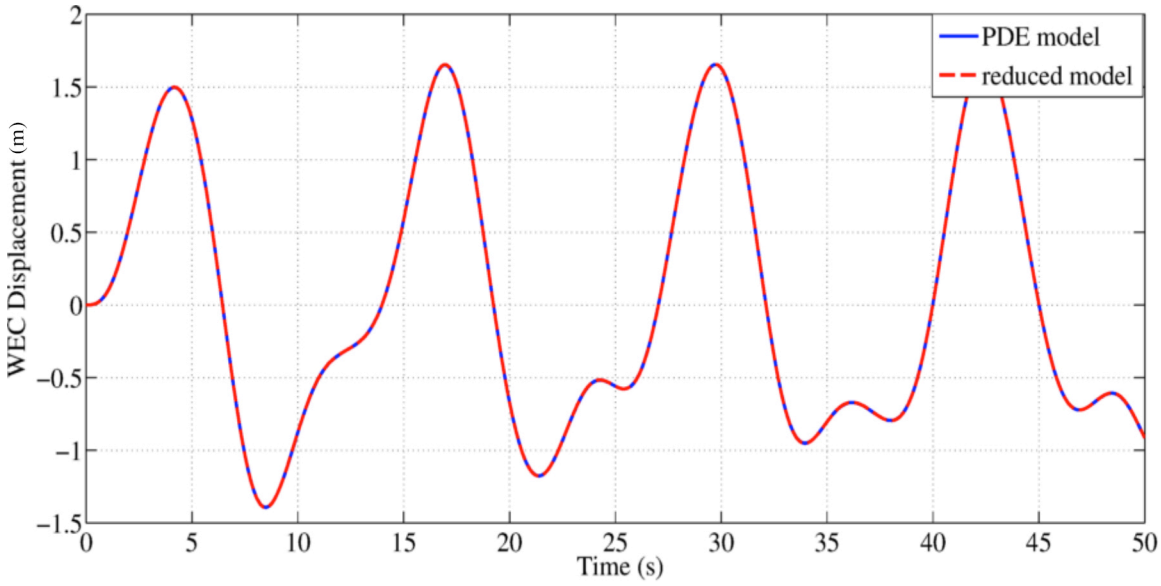

Figure 3.4: Uncontrolled simulation for the displacement of the mass; the figure shows the performance comparison between reduced order model and PDE model for a sinusoidal input function.

Chapter 4: Modeling a Wave Energy Converter in a Wave Tank

As discussed in Chapter 1, the focus of this research is to investigate the suitability of the balanced proper orthogonal decomposition, or Balanced POD, for the fluid-structure interaction arising in WEC dynamics. In this chapter, we present a heuristic model for a wave energy converter in a wave tank, where the waves are generated by a wave maker. We start with a one-dimensional wave equation to model the waves in a wave tank. Appropriate boundary conditions are taken into account on both sides of the tank to best describe the wave maker performance and the motion of the WEC, respectively. The method can be extended to multiple spatial dimensions; however, we shall restrict our attention to the simple 1D PDE model to represent the fluid-structure interaction of the WEC in a wave tank. The following results in this chapter were developed by Singler and can be found in [54].

4.1 Wave Model

To develop a heuristic model of a wave energy converter (WEC) in a wave tank, we consider the following scenario. First, we only consider the waves traveling in the tank in one spatial direction. The wave generator is located at $\xi = 0$, the far wall of the wave tank is located at $\xi = L$, and the WEC is located at $\xi = l$. To develop the heuristic model, we imagine the wave height modeled by the displacement

$w(t, \xi)$ on the spatial interval $0 \leq \xi \leq l$. The waves are generated at the wave generator via a second order oscillator. The WEC at the right end is also modeled as a second order oscillator. Therefore, we arrive at a model that is similar to the second order oscillatory system studied in Chapter 3.

We model the waves by a strongly damped 1D linear wave equation on $0 < \xi < l$

$$w_{tt}(t, \xi) = \gamma w_{t\xi\xi}(t, \xi) + \beta^2 w_{\xi\xi}(t, \xi). \tag{4.1}$$

Other models such as an undamped wave equation or a shallow water equation may be realistic; however, we begin by investigating model reduction of this simpler model and leave other models to be considered in future work. In the equation above and in the remainder of the model below all of the coefficients are nonnegative constants.

We model the wave generator at $\xi = 0$ as an undamped mass-spring system with external force input $f(t)$

$$m_0 w_{tt}(t, 0) = -k_0 w(t, 0) + (\gamma w_{t\xi}(t, 0) + \beta^2 w_{\xi}(t, 0)) + f(t), \tag{4.2}$$

where k_0 denotes the spring stiffness constant corresponding to the wave maker. The term in the parentheses is the force of the wave acting on the mass. We model the motion of the WEC in a similar way; however, we now include both a linear and nonlinear spring force to account for the variety of forces acting on the WEC

(e.g., excitation, radiation, buoyancy) and a control input $u(t)$

$$m_l w_{tt}(t,l) = -k_{l,1} w(t,l) - k_{l,2}[w(t,l)]^3 - (\gamma w_{t\xi}(t,l) + \beta^2 w_\xi(t,l)) + u(t) \tag{4.3}$$

in which $k_{l,1}$ and $k_{l,2}$ are the spring stiffness constants with the latter indicating the nonlinear effects of the spring force. As before, the term in the parentheses is the force of the wave acting on the WEC. At the wall of the wave tank, we impose a partially absorbing boundary condition

$$\alpha_L w_t(t,L) + (\gamma w_{t\xi}(t,L) + \beta^2 w_\xi(t,L)) = 0. \tag{4.4}$$

In order to properly formulate the model above, we need to consider two separate wave equations on the spatial intervals $0 \leq \xi \leq l$ and $l \leq \xi \leq L$ with a coupling condition at $\xi = l$. Instead, we simplify the model and only consider the waves on the spatial interval $0 \leq \xi \leq l$. In order to account for the damping that would occur due to the partially absorbing boundary condition at $\xi = L$, we simply add a damping term $\gamma_l w_t(t,l)$ to the WEC equation of motion as follows

$$m_l w_{tt}(t,l) = -k_{l,1} w(t,l) - k_{l,2}[w(t,l)]^3 - \gamma_l w_t(t,l) - (\gamma w_{t\xi}(t,l) + \beta^2 w_\xi(t,l)) + u(t). \tag{4.5}$$

Therefore, the final model is the 1D wave equation (4.1) on the spatial interval $0 \leq \xi \leq l$, the wave generator boundary condition (4.2), and the damped WEC boundary condition (4.5).

4.2 Energy Function

To ensure that the model developed in the previous section has converging behavior, we look at its energy function. The energy function $E(t)$ at time $t > 0$ associated with a smooth solution w of this WEC-wave system is given by

$$E(t) = \frac{1}{2}\int_0^l \beta^2[w_\xi(t,\xi)]^2 + [w_t(t,\xi)]^2 d\xi + \frac{k_0}{2}[w(t,0)]^2 + \frac{m_0}{2}[w_t(t,0)]^2 + \frac{k_{l,1}}{2}[w(t,l)]^2 + \frac{k_{l,2}}{4}[w(t,l)]^4 + \frac{m_l}{2}[w_t(t,l)]^2. \quad (4.6)$$

Below, we show that if w is a smooth solution and $u = f = 0$, then $E'(t) \leq 0$. This result matches physical intuition and also provides us with the correct energy inner product for the system.

To prove $E'(t) \leq 0$, differentiate $E(t)$ to obtain

$$E'(t) = \int_0^l [\beta^2 w_\xi w_{t\xi} + w_t w_{tt}] d\xi + [m_0 w_{tt}(t,0) + k_0 w(t,0)] w_t(t,0) + [m_l w_{tt}(t,l) + k_{l,1} w(t,l) + k_{l,2} w^3(t,l)] w_t(t,l). \quad (4.7)$$

The wave equation (1) and the boundary conditions (2) and (3) give

$$E'(t) = \beta^2 \int_0^l [w_\xi w_{t\xi} + w_t w_{tt}] d\xi + \gamma \int_0^l w_t w_{t\xi\xi} d\xi + [\gamma w_{t\xi}(t,0) + \beta^2 w_\xi(t,0)] w_t(t,0) - [\gamma_l w_t(t,l) + \gamma w_{t\xi}(t,l) + \beta^2 w_\xi(t,l)] w_t(t,l). \quad (4.8)$$

Next, use $(w_t w_\xi)_\xi = w_\xi w_{t\xi} + w_t w_{\xi\xi}$ to evaluate the first integral and integrate by

parts in the second integral to obtain

$$E'(t) = \beta^2[w_\xi w_t]_{\xi=0}^{\xi=l} + \gamma[w_{t\xi} w_t]_{\xi=0}^{\xi=l} - \gamma \int_0^l [w_{t\xi}]^2 d\xi + [\gamma w_{t\xi}(t,0) + \beta^2 w_\xi(t,0)] w_t(t,0)$$
$$- [\gamma_l w_t(t,l) + \gamma w_{t\xi}(t,l) + \beta^2 w_\xi(t,l)] w_t(t,l). \quad (4.9)$$

this gives

$$E'(t) = -\gamma_l [w_t(t,l)]^2 - \gamma \int_0^l [w_{t\xi}]^2 d\xi \quad (4.10)$$

and therefore $E'(t) \leq 0$. Note that this result holds even if one of the damping constants γ or γ_l equals zero.

4.3 Second Order Abstract Formulation

Following ideas in [10], we rewrite the linearized problem (with $k_{l,2} = 0$) as a second order differential equation

$$\ddot{q}(t) + A_1 \dot{q}(t) + A_0 q(t) = B_0 u(t) + B_1 f(t) \quad (4.11)$$
$$y(t) = C_0 q(t) \quad (4.12)$$

holding over an infinite dimensional Hilbert space. Later, we use this formulation to arrive at a first order formulation of the problem, which we use in the Balanced POD model reduction algorithm. Below, we set notation, specify the Hilbert space, and then define the operators $(A_0, A_1, B_0, B_1, C_0)$.

Let $L^2(0,l)$ be the Hilbert space of (Lebesgue measurable) square integrable

functions defined on $0 \leq \xi \leq l$ with inner product $(f,g)_{L^2} = \int_0^l f(\xi)g(\xi)d\xi$. Let $H^m(0,l)$ denote the Sobolev space of functions $f \in L^2(0,l)$ such that f is m times (weakly) differentiable and each derivative is back in $L^2(0,l)$. Functions in $H^m(0,l)$ must be continuous.

The WEC-wave system can be placed in the second order form with the following variables: the displacement $w(t,\xi)$ function for the wave height on $0 < \xi < l$, and the positions $w_0(t)$ and $w_l(t)$ two masses at $\xi = 0$ and $\xi = l$, respectively.

Let H_0 be the real Hilbert space $H_0 = L^2(0,l) \times R^2$ with the inner product of $x = [w, w_0, w_l] \in H_0$ given by

$$(x,z)_{H_0} = \int_0^l wpd\xi + m_0 w_0 p_0 + m_l w_l p_l. \tag{4.13}$$

Let $V_0 \subset H_0$ be the set of elements

$$x = [w, w_0, w_l] \in H^1(0,l) \times R^2 \tag{4.14}$$

satisfying the compatibility conditions

$$w(0) = w_0, \quad w(l) = w_l. \tag{4.15}$$

For $x = [w, w_0, w_l] \in V_0$ and $z = [p, p_0, p_l] \in V_0$, and the V_0 inner product of x with z is given by

$$(x,z)_{V_0} = \int_0^l \beta^2 w_\xi p_\xi d\xi + k_0 w_0 p_0 + k_{l,1} w_l p_l. \tag{4.16}$$

These inner products were motivated by the energy function considered above.

With this inner product, V_0 is a real Hilbert space. We sketch a proof. First, if $(x,x)_{V_0} = 0$ then $w(\xi)$ is a constant and $w_0 = w_l = 0$. The compatibility conditions imply $w(\xi) = 0$ for all ξ, and so $x = 0$. It is clear that $(.,.)_{V_0}$ satisfies the remaining properties of an inner product.

Next, let $\{x^n\} \subset V_0$ be Cauchy sequence. For $x^n = [w_n, w_0^n, w_l^n]$, we have that $[w_\xi^n, w_0^n, w_l^n]$ is a Cauchy sequence in $L^2(0,l) \times R^2$. Therefore, there exists $[z, w_0, w_l] \in L^2(0,l) \times R^2$ such that

$$w_\xi^n \to z \quad \text{in} \quad L^2(0,l), \quad w_0^n \to w_0, \quad w_l^n \to w_l. \tag{4.17}$$

Define w by $w(\xi) = w_0 + \int_0^\xi z(\eta)d\eta$. Then $w \in H^1(0,l)$, $w_\xi = z$, and $w(0) = w_0$. Also, we have $w(l) = w_l$ since

$$w(l) = \lim_{n\to\infty} w_0^n + \int_0^l w_\xi^n(\eta)d\eta = \lim_{n\to\infty} w_l^n = w_l. \tag{4.18}$$

Therefore w satisfies both compatibility conditions and x^n converges in V_0 to $x = [w, w_0, w_l] \in V_0$. This proves V_0 is a Hilbert space.

Next, define the unbounded operator $A_0 : D(A_0) \subset H_0 \to H_0$ as follows. Let $D(A_0)$ be the set of $q = [p, p_0, p_l] \in V_0$ such that $p \in H^2$. For $q \in D(A_0)$, define

$$A_0 q = \begin{bmatrix} -\beta^2 p_{\xi\xi} \\ m_0^{-1}[k_0 p_0 - \beta^2 p_\xi(0)] \\ m_l^{-1}[k_{l,1} p_l + \beta^2 p_\xi(l)] \end{bmatrix}. \tag{4.19}$$

The definition of the operator A_1 depends on the constant γ. If $\gamma = 0$, then $A_1 : H_0 \to H_0$ is a bounded operator and $A_1 q$ for $q = [p, p_0, p_l] \in H_0$ is given by

$$A_1 q = \begin{bmatrix} 0 \\ 0 \\ m_l^{-1}\gamma_l p_l \end{bmatrix} \tag{4.20}$$

where, again, $q = [p, p_0, p_l]$. Finally, define the bounded operators $B_0 : R \to H_0$, $B_1 : R \to H_0$ and $C_0 : V_0 \to R$ as follows:

$$B_0 u = \begin{bmatrix} 0 \\ 0 \\ m_l^{-1} u \end{bmatrix}, \quad B_1 f = \begin{bmatrix} 0 \\ m_0^{-1} f \\ 0 \end{bmatrix} \tag{4.21}$$

and

$$C_0 q = p(\xi) \tag{4.22}$$

for $q = [p, p_0, p_l]$ and $0 < \xi < l$ for observing wave height at a location ξ between the wave generator and the WEC, or

$$C_0 q = p(l) \tag{4.23}$$

for observing wave height at the WEC. This completely specifies the formulation of the second order differential equation (4.11).

4.4 First Order Abstract Formulation

To apply the Balanced POD model reduction algorithm to this system, we rewrite the second order system (4) in first order form as

$$\dot{x}(t) = Ax(t) + Bu(t) + Df(t), \tag{4.24}$$

$$y(t) = Cx(t) \tag{4.25}$$

where (A, B, D, C) are operators acting on the Hilbert space $H = V_0 \times H_0$ with inner product $([w, v], [p, q])_H = (w, v)_{V_0} + (p, q)_{H_0}$. This formulation can be used along with simulation techniques such as finite elements in order to produce a reduced order model using Balanced POD.

Define the operator $A : D(A) \subset H \to H$, where $D(A) = D(A_0) \times V_0$ if $\gamma = 0$ and $D(A) = D(A_0) \times D(A_0)$ if $\gamma > 0$, by

$$Ax = \begin{bmatrix} 0 & I \\ -A_0 & -A_1 \end{bmatrix}. \tag{4.26}$$

Also define the bounded operators $B : R \to H$, $D : R \to H$ and $C : H \to R$ by

$$Bu = [0, B_0 u]^T, \quad Df = [0, B_1 f]^T, \quad C[w, v] = C_0 w. \tag{4.27}$$

This determines the linear system (4.24).

For the Balanced POD algorithm, we provide alternate expressions for B, D

and C as follows. Define $b, d, c \in H$ by

$$b = [0, 0, 0, 0, 0, m_l^{-1}], \quad d = [0, 0, 0, 0, m_0^{-1}, 0], \quad c = [p, p_0, p_l, 0, 0, 0], \tag{4.28}$$

$$p(\xi) = p_0 + l^{-1}(p_l - p_0)\xi, \quad p_0 = wp_l, \tag{4.29}$$

$$p_l = \frac{1}{k_{l,1} + k_0 w} \quad w = \frac{\beta^2}{\beta^2 + k_0 l}. \tag{4.30}$$

It can be checked that we have

$$Bu = bu, \quad Df = df, \quad Cx = (c, x)_H \tag{4.31}$$

for all $u, f \in R$ and $x \in H$.

4.5 Weak Formulation

For Balanced POD, we need to simulate the forward differential equation

$$\dot{x} = Ax(t), \quad x(0) = b, \tag{4.32}$$

and the adjoint differential equation

$$\dot{z} = A^* z(t), \quad z(0) = c, \tag{4.33}$$

where $b, c \in H$ are defined in (4.28). It should be noted that the Balanced POD reduction technique will be applied to the pair of (A, b), assuming that f acts like

disturbance coupled through d matrix. Once the balanced transformation matrix is computed, we will use that to reduce the disturbance matrix.

We focus on simulations for the strongly damped case where $\gamma, \gamma_l > 0$. In this case we can show the problem is parabolic, and therefore we place the equations in weak form and use finite elements for the simulations. This is of course only one simulation technique; many other approximation methods will also yield accurate results.

Define the Hilbert space $V = V_0 \times V_0$ with inner product $([w,v],[p,q])_V = (w,v)_{V_0} + (p,q)_{V_0}$. Let $x = [w,v]$, take the H inner product of the forward differential equation (4.32) with $\chi = [p,q] \in V$, and integrate by parts to obtain the parabolic problem

$$\frac{d}{dt}(x,\chi)_H + a(x,\chi) = 0 \quad \text{for all} \quad \chi \in V. \tag{4.34}$$

Here, the bilinear form $a : V \times V \to R$ is defined by

$$a(x,\chi) = -(v,p)_{V_0} + (v,q)_{V_1} + (w,p)_{V_0} \tag{4.35}$$

for any $x = [w,v] \in V$ and $\chi = [p,q] \in V$. The V_0 inner products result from integrating by parts in the terms involving A_0, and the bilinear form $(.,.)_{V_1}$ is obtained by integrating by parts in $(A_1 v, q)_{H_0}$ to obtain

$$([f,f_0,f_l],[g,g_0,g_l])_{V_1} = \int_0^l \gamma f_\xi g_\xi d\xi + \gamma_l f_l g_l, \tag{4.36}$$

where $v = [f, f_0, f_l]$ and $q = [g, g_0, g_l]$.

Now take $\chi = [p, 0] \in V$ and $\chi = [0, q] \in V$ to obtain

$$\frac{d}{dt}(w, p)_{V_0} = (v, p)_{V_0} \quad \text{for all} \quad p \in V_0 \tag{4.37}$$

and

$$\frac{d}{dt}(v, p)_{H_0} = -(w, q)_{V_0} - (v, q)_{V_1} \quad \text{for all} \quad q \in V_0. \tag{4.38}$$

These equations can be used to approximate the solution of the forward differential equation (4.32) using finite element methods or other Galerkin methods.

Since the problem is parabolic, the weak form of the adjoint differential equation (4.33) is characterized by

$$\frac{d}{dt}(z, \chi)_H + a(\chi, z) = 0 \quad \text{for all} \quad \chi \in V. \tag{4.39}$$

Note that the arguments of the bilinear form a have been switched compared to the forward problem (9). Let $z = [w, v]$. Taking $\chi = [p, 0] \in V$ and $\chi = [0, q] \in V$ gives

$$\frac{d}{dt}(w, p)_{V_0} = -(p, v)_{V_0} \quad \text{for all} \quad p \in V_0 \tag{4.40}$$

and

$$\frac{d}{dt}(v,q)_{H_0} = (q,w)_{V_0} - (q,v)_{V_1} \quad \text{for all} \quad q \in V_0. \tag{4.41}$$

Again, we can use these equations to approximate the solution of the adjoint differential equation (8).

We note that the problem involving the inputs Bu and Df and the nonlinear term can also be placed in a weak formulation in a similar manner. This weak form can also be used for simulating the nonlinear PDE.

Remark 1: The solution of the adjoint problem will be smoother than the solution of the forward problem. This is due to the smoothness of the initial data. For the forward problem, we have $b \in H = V_0 \times H_0$, but $b \notin V = V_0 \times V_0$ since b does not satisfy the compatibility conditions for the second V_0 space. Specifically, the initial data b corresponds to zero initial displacement everywhere, the wave generator mass (at $\xi = 0$) having a nonzero initial velocity, and zero initial velocity elsewhere. For the adjoint problem, the initial data satisfies $c \in V$. Since the initial data is smooth and satisfies all compatibility conditions, the solution $z(t)$ will be easier to approximate than the solution $x(t)$ of the forward problem, which has discontinuous initial velocity.

Chapter 5: Experiments and Simulation Results

In this chapter, we present the numerical results regarding applying Balanced POD algorithm to the finite element approximation of the model problem for the two different wave height sensor locations described in Chapter 4. We then present simulations of the system behavior for the uncontrolled and controlled cases. In the controlled case, the tracking control of the reduced order system will be addressed with the aim of maximizing the power output of the WEC using the two well-known optimal control strategies, namely Linear Quadratic Regulator (LQR) and Linear Quadratic Gaussian (LQG) controllers. The last experiment will be dedicated to determining the underlying ocean wave function in order for the WEC to track. This experiment gives insight into the tracking function that the WEC is required to follow.

5.1 Formulating the Finite Element Approximation

First, we apply a finite element method for the spatial discretization in order to obtain an approximation to the model problem in (4.1), (4.2) and (4.5). Then, Balanced POD is applied to the approximating system to obtain a reduced order system of order r. Finally, we form the resulting reduced order system so that an optimal controller can be designed for the WEC.

Following the process outlined in Chapter 4, a Galerkin-based finite element approximation is applied to the WEC wave system developed in (4.1), (4.2) and (4.5). Taking N as the number of linear B-splines in the interval $[0, l]$ (indicating the dimension of the approximating space $w^N \subseteq w$), we obtain the first order system

$$\dot{x}^N = A^N x^N + B^N u + D^N f + N^N(x^N(t)), \quad x^N(0) = x_0^N \tag{5.1}$$

with two possible outputs

$$y_1(t) = C_1 x^N(t) \quad \text{or} \quad y_2 = C_2 x^N(t) \tag{5.2}$$

Here, C_2 represents the case where the wave height measurement is made in the middle of the wave tank, and C_1 represents the case where the wave height is measured at the WEC. The state vector is given by $x^N(t) = [q^N(t), \dot{q}^N(t)]^T$ and

$$A^N = \begin{bmatrix} 0 & I \\ -M^{-N}K^N & -M^{-N}L^N \end{bmatrix}, \tag{5.3}$$

$$B^N = \begin{bmatrix} 0 \\ M^{-N}B_0^N \end{bmatrix} \quad D^N = \begin{bmatrix} 0 \\ M^{-N}D_0^N \end{bmatrix} \tag{5.4}$$

$$N^N(x^N(t)) = \begin{bmatrix} 0 \\ -M^{-N}N_0^N(q_N(t)) \end{bmatrix} \tag{5.5}$$

$$C_1 = [0_{1\times N-1} \quad 1 \quad 0_{1\times N}], \quad C_2 = [0_{1\times(\frac{N}{2}-1)} \quad 1 \quad 0_{1\times\frac{N}{2}} \quad 0_{1\times N}] \tag{5.6}$$

$$[M^N]_{ij} = \int_0^l b_i(\xi)b_j(\xi)d\xi + m_0 b_i(0)b_j(0) + m_l b_i(l)b_j(l), \tag{5.7}$$

$$[L^N]_{ij} = \int_0^l \gamma b_i'(\xi)b_j'(\xi)d\xi + \gamma_l b_i(l)b_j(l) \tag{5.8}$$

$$[K^N]_{ij} = \int_0^l \beta^2 b_i'(\xi)b_j'(\xi)d\xi + k_0 b_i(0)b_j(0) + k_1 b_i(l)b_j(l), \tag{5.9}$$

$$B_0^N = [0_{1\times 2N-1} \quad 1], \quad D_0^N = [1 \quad 0_{2\times 2N}] \tag{5.10}$$

$$N_0^N(q(t)) = k_2 q_N^3(t) \tag{5.11}$$

In order to compute the high order system, the parameters in Table 5.1 are chosen.

Table 5.1: Simulation Parameters

Parameter	Value
Wave tank length(l)	$5m$
WEC mass (m_l)	$1kg$
Wave maker mass (m_0)	$1.5kg$
γ	0.005
γ_l	0.005
β	1
$k_{l,1} = k_{l,2}$	1
k_0	1

5.2 Applying Balanced POD

The Balanced POD algorithm is applied to the finite element approximation of the model problem to obtain a low order model. It is important not only to choose a low order system of size r that approximates the high order system well, but it is important to begin with a refined enough high order system that is "converged" to the original distributed parameter model. In Fig. 5.1, we show the approximate Hankel singular values for $N = 80, 160$, and 320 for each of the systems given by C_1 and C_2. Notice, for this problem, the order of the system, is $2N$; there are N states representing the system displacements, and N representing the system velocities. Notice the convergence of singular values with mesh refinement.

Based on the convergence shown in the plots above, the approximating system arising from $N = 160$ basis functions (and 320 states) was chosen as the "high order system". To determine the size of reduced order system that would be used for the control computations, we computed the error in system approximation for various values of r. Those are shown for the two systems in Table 5.2 below.

We note that the error is within one order of magnitude for all choices of r. So for the remainder of the simulations, we use the reduced order models for the systems corresponding to C_1 and C_2 of order 20. Also note that $r = 20$ is the number of states in the reduced order system, analogous to 320 states in the full order system.

To compare the input-output response of the nonlinear PDE and the nonlinear reduced order models, uncontrolled simulations are performed to show the per-

Table 5.2: Balanced POD error for various r values for two system configurations

system	$r = 6$	$r = 20$	$r = 40$
BPOD error for C_1	9.749×10^{-1}	1.35×10^{-2}	1.107×10^{-4}
BPOD error for C_2	1.9922	1.126×10^{-1}	3.2×10^{-3}

formance of the reduction method. In all simulations, the forcing function at the wave generator was chosen to be $f(t) = \sin(0.2\pi t) + \eta$ where η was selected to be a Gaussian noise signal with mean 0, variance 0.1 multiplied by a factor of 1/20. The noise was selected through a trial and error process to create a wave that had a slight amount of irregularity to it. The system was started from a resting position.

Fig. 5.2 illustrates the displacement of the WEC under this forcing function. Notice that the WEC does not move until $t = X$ when the wave reaches the WEC at $l = 5m$.

We note that both reduced order systems compare quite well to the high order approximation to the nonlinear distributed parameter system. The system in which the wave height is measured at mid-tank is slightly less accurate, which might be expected as the error in the balanced POD approximation was larger than for the system in which the wave height was measured at the WEC.

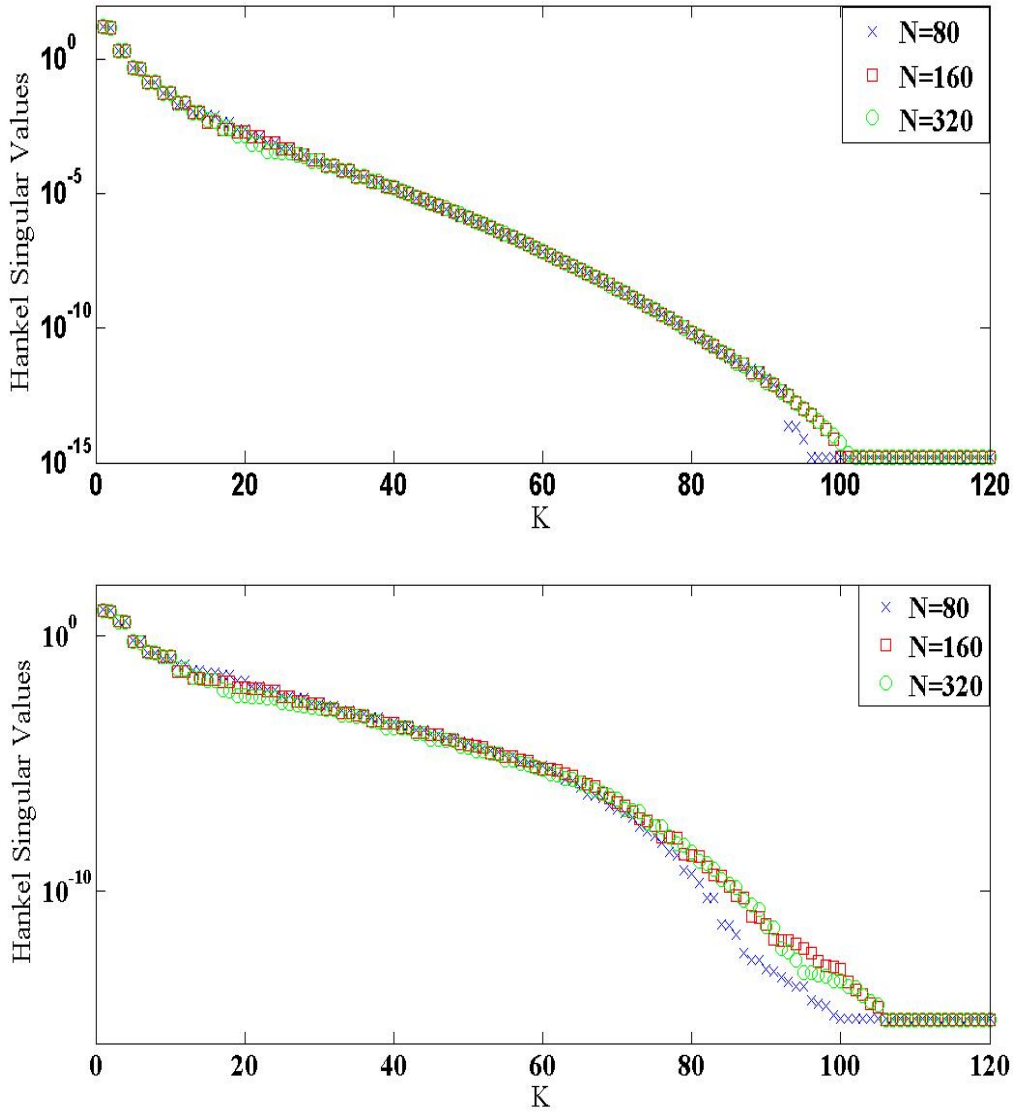

Figure 5.1: Approximate Hankel Singular Values for system with wave measurement i) at WEC (top), ii) midway between wave maker and WEC (bottom)

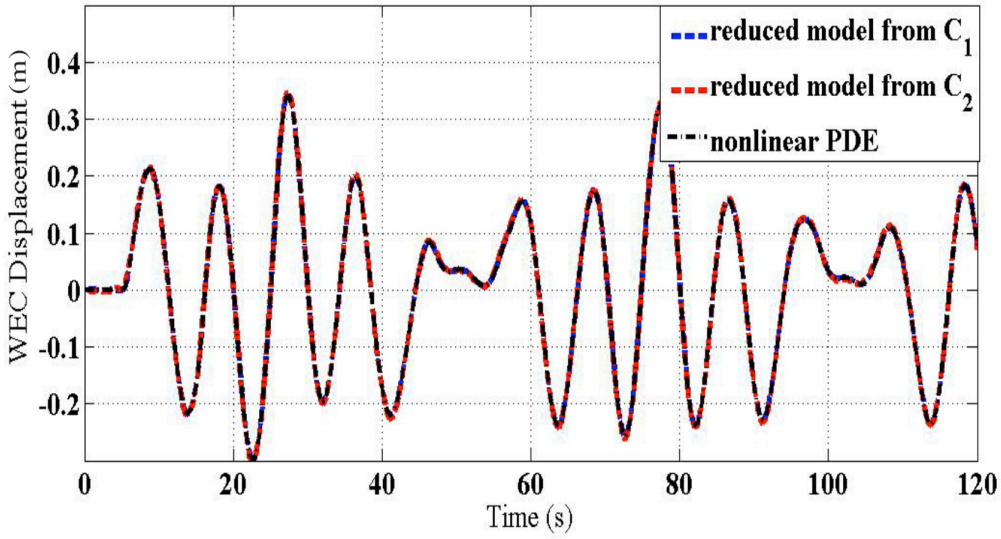

Figure 5.2: Uncontrolled response of nonlinear high order system vs. nonlinear reduced models; The reduced order systems compare quite well to the high order approximation.

5.3 Feedback Control for the Reduced Order Model

As discussed earlier, as wave energy converter (WEC) technologies mature, designing effective control strategies to extract maximum energy, extend device life, coordinate WEC operation within an array, or mitigate negative impacts of extreme forces on a WEC becomes an increasingly important area of research. To achieve many of these goals, tracking controls are often implemented. In the following computations, we will implement a standard Linear Quadratic Regulator with tracking and Linear Quadratic Gaussian (LQG) controller, not because they are meant to be the most effective or desirable of control approaches, but because they are simply illustrative of the nature of a tracking control that might be applied to this problem.

5.3.1 LQR Control

In the LQR control problem (found, for example, in [55]), an optimal control solution is found by minimizing the cost function defined as

$$J(u) = \int_0^\infty (x^T(t)Qx + u^T Ru)dt \tag{5.12}$$

where $x(t)$ is the state vector, u is the control input, Q, R are weighting matrices. There exists an optimal control solution of the form

$$u(t) = -R^{-1}B^T\Pi x(t) = -Kx(t) \tag{5.13}$$

where Π is the solution to the control algebraic Riccati equation

$$A^T + \Pi + \Pi A - \Pi B R^{-1} B^T \Pi + Q = 0. \tag{5.14}$$

For the LQR tracking control of the WEC, we choose the desired state to have the same frequency as the forcing function at the wave generator with a relatively smaller amplitude

$$w^N(t, l) = 0.3 \sin(0.2\pi t). \tag{5.15}$$

The state weighting matrix in the control objective function is chosen to be zero for states that do not correspond to the WEC position, and 1 for WEC position. Therefore, this tracking control should serve to drive the WEC into the periodic behavior desired.

In Fig. 5.3, we show the behavior of the high order uncontrolled system, the tracking function, and the reduced order controlled system with the wave measurement taken midtank. Here one can see that the tracking function is trying to roughly preserve the phase of the oscillations, and drive the WEC toward the peaks of the uncontrolled behavior. Again, there is nothing physically relevant about this choice of tracking function; it is merely representative of the types of controls that can be found in the literature. To compare the performance of the controlled high order system with the controlled reduced order systems, we refer to Fig. 5.4. Here, we again see little difference in the performance of the high order system with the reduced order systems. All systems perform in a qualitatively acceptable manner. As shown in Figure 5.4, the controlled WEC in C_2 system

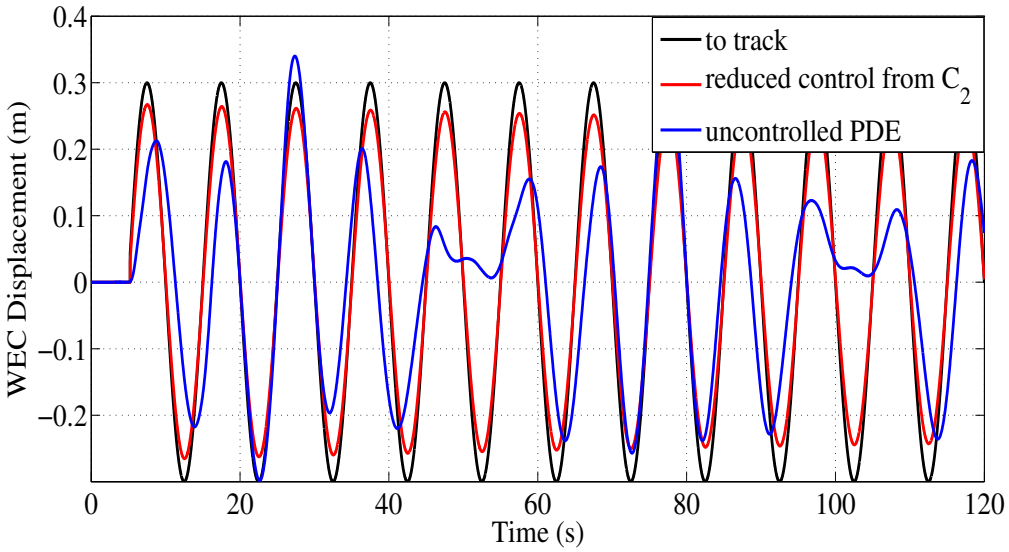

Figure 5.3: Performance comparison between controlled and uncontrolled systems with wave measurement midway between wave maker and WEC

(where the wave height is measured midway) slightly outperforms the controlled WEC in C_1 system (where the wave height is measured at the WEC). This is due to the fact that C_2 system provides an estimation of the ocean state to the WEC prior to the tracking control problem. In other words, by having a wave buoy operating at a distance to WEC, we can estimate the underlying ocean wave function in order for the WEC to track using wave height data. We will further present a method to construct the tracking function from wave height measurements in the upcoming sections. The amount of control used in both system configurations to create such tracking performance is depicted in Figure 5.5.

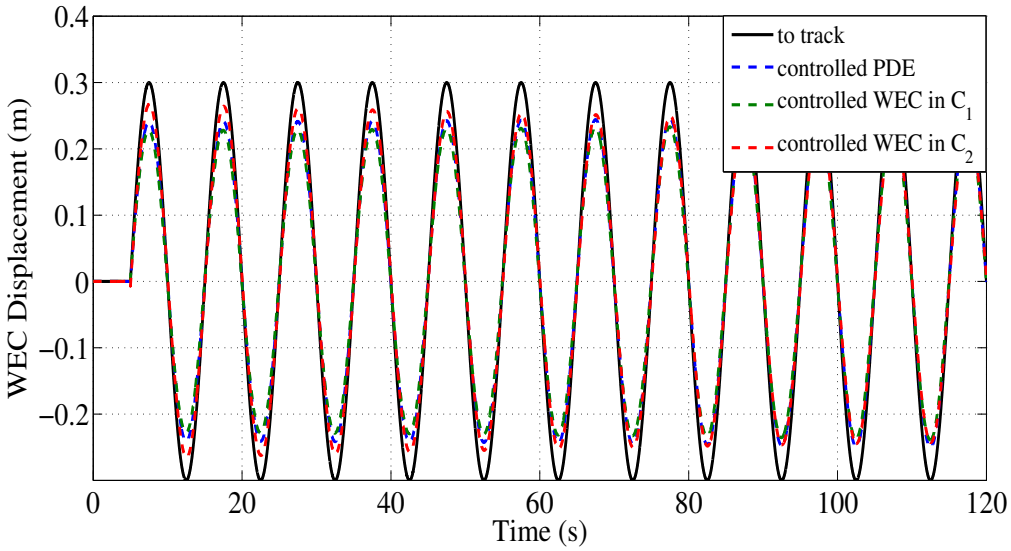

Figure 5.4: Performance comparison between finite element system and both reduced systems

5.3.2 LQG Control

One issue with LQR control is that it requires the full knowledge of all the states for all times. So there is a problem with implementing a full state feedback control that seems to be impractical. An alternative to this control method is Linear Quadratic Gaussian (LQG) compensator.

Given the system measurements $y(t)$, the optimal estimator (LQG) attempts to find a dynamical system that is able to estimate the states of the system $x(t)$. The dynamics of the estimator is represented as

$$\dot{x}_c(t) = A_c x_c(t) + F y(t) \quad x_c(0) = x_{c_0} \tag{5.16}$$

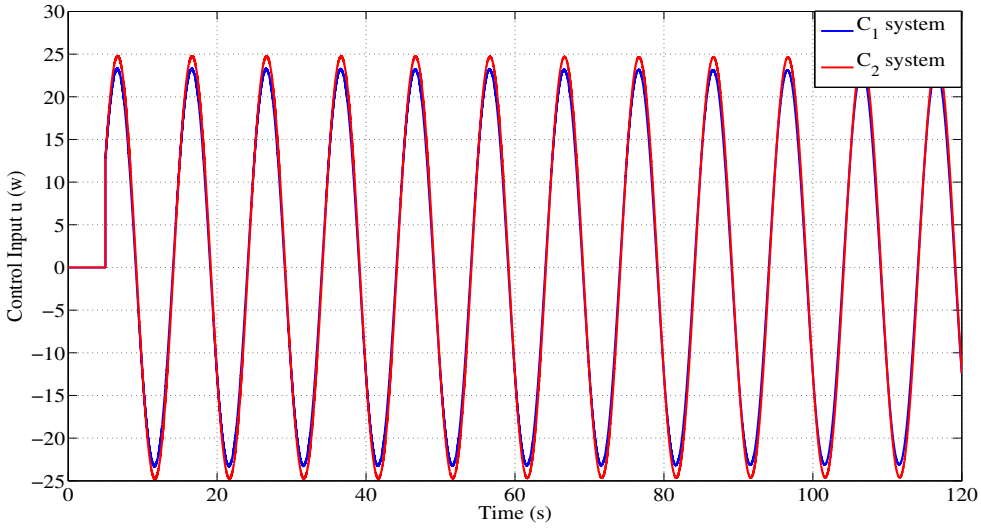

Figure 5.5: Control inputs used in LQR problem for both system configurations: note that the control system does not start until the first wave hits the WEC.

$$u(t) = -Kx_c(t). \tag{5.17}$$

By inserting the linear feedback control law into the system, we get the closed-loop system as

$$\begin{bmatrix} \dot{x}(t) \\ \dot{x}_c(t) \end{bmatrix} = \begin{bmatrix} A & -BK \\ FC & A_c \end{bmatrix} \begin{bmatrix} x(t) \\ x_c(t) \end{bmatrix} \tag{5.18}$$

in which A_c, F and K are found by solving the control algebraic Riccati equation and the filter algebraic Riccati equation

$$AP + PA^T - PC^TCP + M = 0 \tag{5.19}$$

then

$$K = R^{-1}B^T\Pi, \quad F = PC^T \tag{5.20}$$

$$A_c = A - BK - FC. \tag{5.21}$$

In order to design a LQG controller that is able to track a reference trajectory, an integral action is added to the feedback control system. The integral action aims at minimizing the error between the output and the desired state. Figure 5.6 shows the block diagram of the LQG control system with integral action. For the LQG

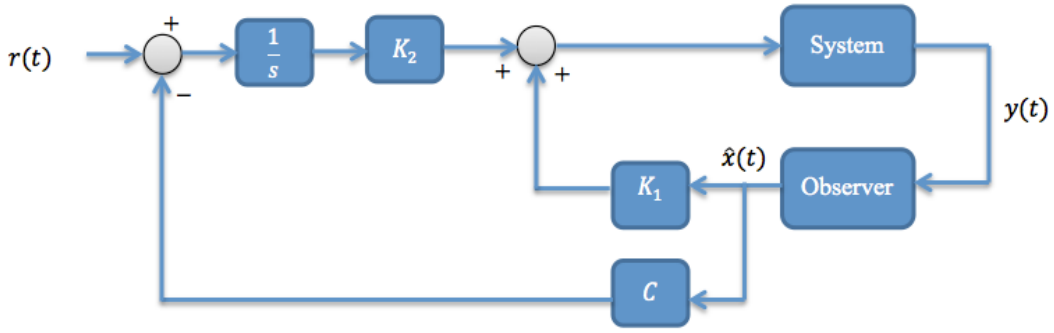

Figure 5.6: LQG control with integral action

control of the WEC, we again use the desired state $w^N(t,l) = 0.3\sin(0.2\pi t)$. The performance of the LQG control is shown in Figure 5.7. In this case, the amount of control that we are using to create a tracking performance via an estimator is illustrated in Figure 5.8.

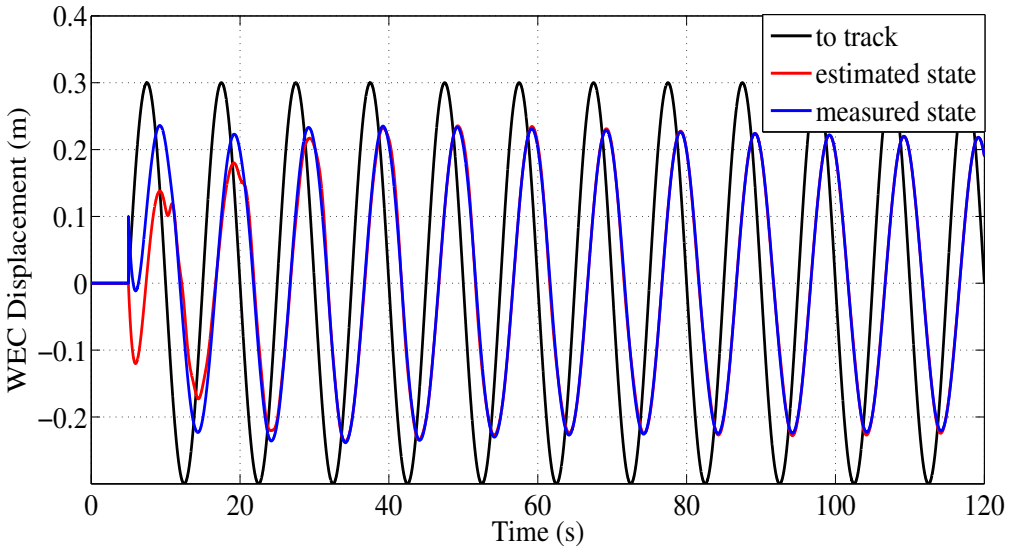

Figure 5.7: LQG control of the WEC in C_1 system

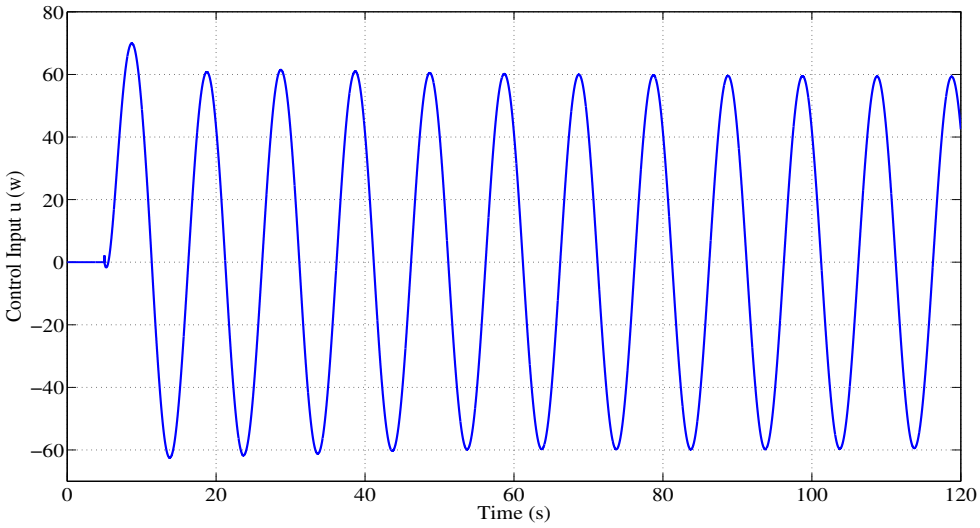

Figure 5.8: The amount of control used in LQG problem

5.4 Estimating Underlying Ocean Function

In the previous section, two feedback control strategies were implemented in order for the WEC to track the underlying ocean function so that the WEC remains close to resonance with the incident irregular wave field. These implementations were based on the fact that the underlying ocean function that serves as the tracking function for the control system is known to us. However, the assumption of knowing what the WEC is going to track seems unrealistic.

In this experiment, we will implement a method for estimating the tracking function based on sensor measurements that is used for the control system. The problem of constructing the ocean state based on sensor measurements has been addressed and can be found in literature [56, 57]. The wave height data provided by wave buoys at some location away from WEC can be used to estimate the incoming ocean state to the WEC.

Of the various interesting methods for treating the complex ocean waves is the spectral analysis. The spectral is based on the Fast Fourier Transform of the sea surface [56]. This method assumes that the sea state can be reconstructed by a summation of a large number of sinusoidal functions with various frequencies and heights. The Fourier Transform applied to a set of recorded wave height data provides the wave spectrum that is useful for indicating that what frequencies within the ocean waves have significant energy content.

To do so, we first measure time series wave height data at location midway between the wave maker and the WEC and then record the data as $w(\bar{s}, t)$, where

$\bar{s}$ denotes the mid point.. Figure 5.9 shows the time series profile for 10 minute of data. Note that we use the wave maker to create the incident waves here.

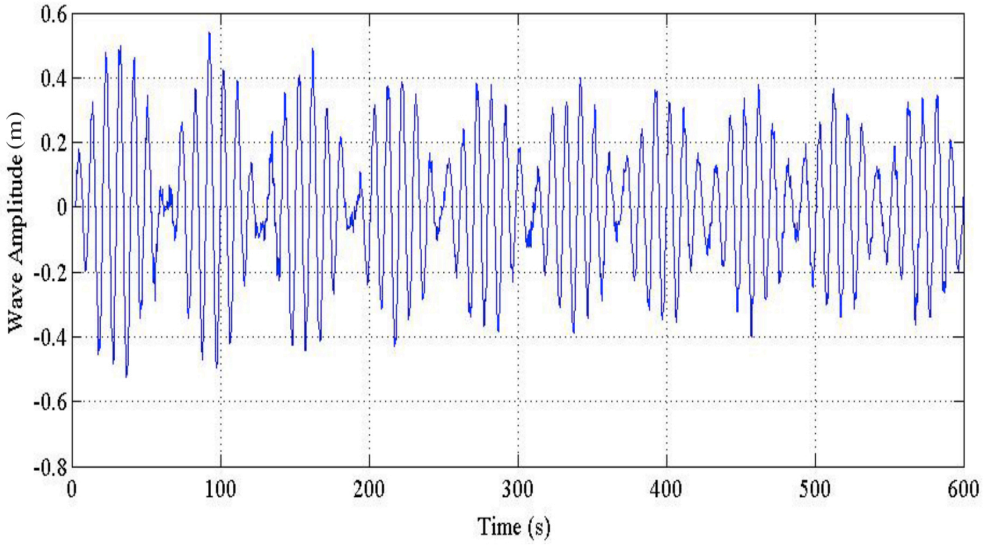

Figure 5.9: 10 minute record of wave amplitude measured by a wave buoy

Now we can perform Fast Fourier Transform on the data to convert it to the frequency domain. In the frequency domain, the most dominant frequency should be the peak of the spectral curve. The wave spectrum of the above time series wave height data is illustrated in Figure 5.10. As seen in Figure 5.10, the peak wave frequency and peak wave period are $f_p = 0.105$ and $T_p = 9.3091$. The spectral analysis of the ocean wave would help us to find an approximation to the ocean state, which in turn will give us the tracking function that the WEC is required to track in order to be in resonant with ocean waves. The approximated ocean state

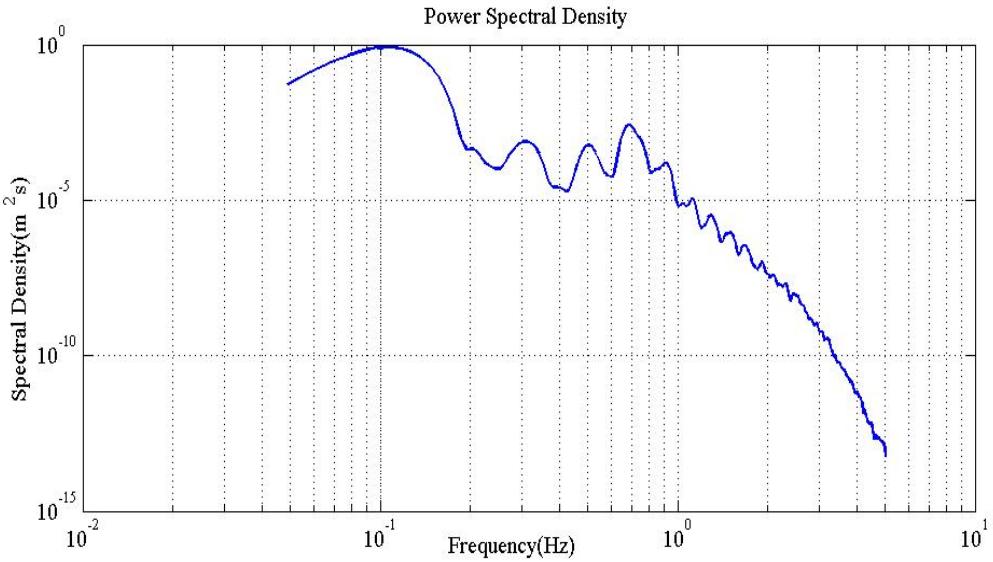

Figure 5.10: The spectrum of 10 minute ocean wave height data

can be computed using

$$\hat{w}(t,l) = \sum_{n=1}^{\infty} \sqrt{2S(n)} \sin(2\pi n f t) \tag{5.22}$$

where f is the fundamental frequency extracted from the wave spectrum and $S(n)$ denotes the spectrum of the ocean wave defined as

$$S(n) = Z_n Z_n^* \tag{5.23}$$

where

$$Z_n = \frac{1}{T} \int_{-T/2}^{T/2} \hat{w}(t,l) \sin(2\pi n f t) dt \tag{5.24}$$

for a period of T.

This method can be applied to real ocean wave data taken from ocean buoys. The wave data used here is obtained from a Datawell Directional Waverider buoy located at the Belmullet Wave Energy Test Site on the western coast of Ireland. The depth at the buoy location is 50 m and is located about 2 nm from shore. An accelerometer records data in the heave direction at 1.28 Hz, and is double integrated to obtain surface displacement. In Figure 5.11, 20 minutes of recorded wave height data at 1.28 Hz, the recording frequency of the actual buoy data is shown.

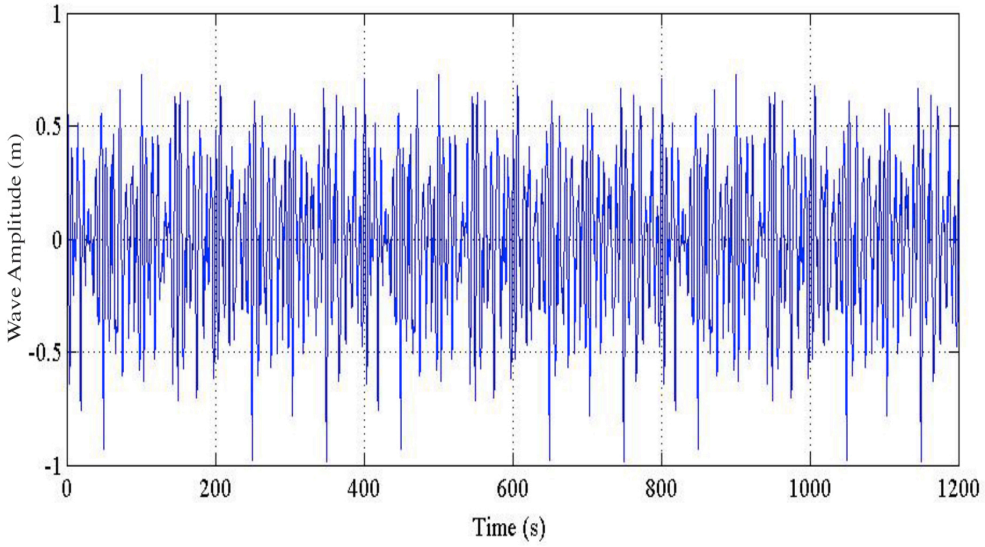

Figure 5.11: 20 minutes of recorded wave height data from an ocean buoy

Performing the FFT on the wave data yields the wave spectrum from which we can reconstruct the tracking function, as shown in Figure 5.12. According to this figure, the dominant wave frequency is $f_p = 0.1313$. The sea state can

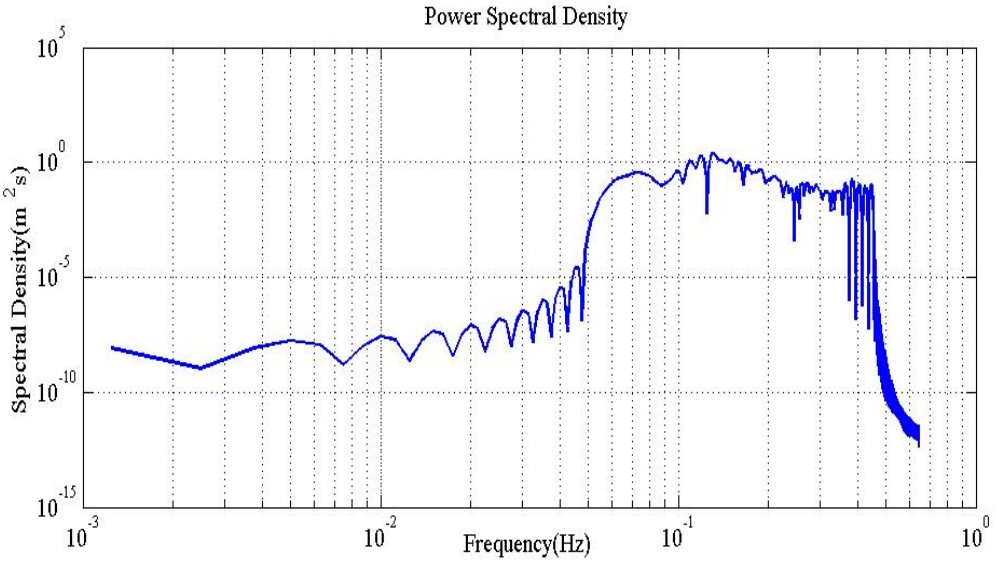

Figure 5.12: The spectrum of 20 minute ocean wave height data from the ocean buoy

be reconstructed in the same way as the previous ocean wave data. In other words, one can easily estimate the underlying ocean wave function by obtaining this information in order to design tracking controllers for WECs.

Chapter 6: Conclusion

The work presented in this thesis has investigated the application of a model reduction technique to wave energy conversion problem. Due to the complex fluid-structure interactions of the WEC in the ocean and the forces on the WEC, a high fidelity model could be replaced by a more tractable and computationally efficient models. Thus, reduced-order models can be readily used for real-time computation of WEC control systems. Among various model reduction approaches, Balanced POD has received much attention in recent years, as previously discussed in Section 3.1. Although Balanced POD has been utilized for model reduction of a variety of complex systems, the method was tested in the context of Hyperbolic systems in Chapter 3 to ensure its applicability for the WEC fluid-structure interaction problem and to provide the overview of the approach.

The suitability of Balanced POD to the WEC dynamics that has been the underlying purpose of this work, presents a great promise into the replacement of high-fidelity models with reduced-order ones for real-time control. More specifically, as provided in Chapter 5, a high-dimensional system of order 320×320 resulting from the application of a finite dimensional scheme to the WEC dynamics in a wave tank was replaced by a reduced order model of order 20. The results produced in Section 5.2 clearly show the necessity of using a model reduction approach for real-time control design.

Once the reduced-order model was sought, the feedback control of the WEC was introduced in Section 5.3 with the purpose of keeping the WEC as close as possible to resonance with the incident irregular ocean waves. In fact, resonance would help to extract maximum energy off the WEC with the minimal amount of the user input. As the first attempt to illustrate the nature of a tracking control problem, we developed LQR tracking control as well as LQG control system in order to drive the WEC into the desired periodic behavior with the information provided in two different system configurations, as discussed in Section 5.3. Furthermore, we proposed a practical method to predict the underlying ocean wave function based on buoy wave height data. We successfully tested the method on both simulation data and real ocean buoy data in Section 5.4 to construct the desired tracking function in order for the WEC to follow.

6.1 Future Work

In this work, we considered a one-dimensional heuristic model for a WEC in a wave tank as the first attempt in a planned series of work that seeks the applicability of Balanced POD for WEC problems. We took a fairly simplified approach in this new domain with the ambition to open up a novel research venue that tries to address the problem of WEC real-time control.

Future work will involve:

1. Extending the aforementioned method to multiple spatial dimensions.

2. Developing the WEC model in the real ocean and taking the stochastic nature

of ocean waves into account.

3. Testing various approaches to state estimation that can be utilized with the information limits inherent in ocean operations.

4. Designing advanced controllers to accomplish more goals besides extracting the maximum energy.

Bibliography

[1] M. Richter, M. E. Magana, O. Sawodny, and T. K. Brekken, "Nonlinear model predictive control of a point absorber wave energy converter," *IEEE Transactions on Sustainable Energy*, vol. 4, no. 1, pp. 118–126, 2013. [Online]. Available: http://dx.doi.org/10.1109/TSTE.2012.2202929

[2] S. R. Nielsen, Q. Zhou, M. M. Kramer, B. Basu, and Z. Zhang, "Optimal control of nonlinear wave energy point converters," *Ocean Engineering*, vol. 72, no. 0, pp. 176 – 187, 2013. [Online]. Available: http://www.sciencedirect.com/science/article/pii/S0029801813002758

[3] L. Knockaert and D. D. Zutter, "Passive reduced order multiport modeling: the padé-laguerre, krylov-arnoldi-svd connection," *International Journal of Electronics and Communications*, pp. 254–260, 1999.

[4] F. Kleibergen and R. Paap, "Generalized reduced rank tests using the singular value decomposition," *Journal of Econometrics*, 2005.

[5] P. Benner and A. Schneider, "Balanced truncation model order reduction for LTI systems with many inputs or outputs," in *Proceedings of the 19th International Symposium on Mathematical Theory of Networks and Systems*, 2010.

[6] C. Rowley, "Model reduction for fluids using balanced proper orthogonal decomposition," *International Journal on Bifurcation and Chaos*, no. 15, pp. 997–1013, 2004.

[7] J. Singler, J. Merritt, C. Ray, and B. A. Batten, "Reduced order controllers for an anisotropic composite plate with smart actuation and sensing," in *American Control Conference (ACC)*, June 2013, pp. 1272–1277.

[8] W. Hu and J. R. Singler, "A modified balanced POD model reduction algorithm for parabolic PDEs with unbounded inputs," in *to appear in Proceedings of 2014 American Control Conference.*, 2014.

[9] J. R. Singler, "Balanced POD for model reduction of linear PDE systems: Convergence theory," *Numerische Mathematik*, vol. 121, no. 1, pp. 127–164, 2012.

[10] J. A. Burns and B. B. King, "A reduced basis approach to the design of low-order feedback controllers for nonlinear continuous systems," *Journal of Vibration and Control*, vol. 4, no. 3, pp. 297–323, 1998.

[11] T. W. Thorpe, "The wave energy program in the UK and the european wave energy network," in *Fourth European Wave Energy Conference*, 2000.

[12] B. Drew, A. Plummer, and M. Sahinkaya, "A review of wave energy converter technology," *Journal of Power and Energy*, vol. 1, 2009.

[13] Centre for Renewable Energy Sources, *Wave Energy Utilization in Europe*, European Thematic Network on Wave Energy.

[14] M. Previsic, "Wave power technologies," *Power Engineering Society General Meeting*, vol. 2, 2005.

[15] M. Andersen, K. Argyriadis, and S. Butterfield, "Ocean wind and wave energy utilization," in *17th International Ship and Offshore Structures Congress*, Seoul, Korea, 2007.

[16] J. Falnes, "A review of wave-energy extraction," *Marine Structures*, vol. 20, pp. 185–201, 2007.

[17] B. Czech, P. Bauer, and H. Polinder, "Review of wave energy converters," in *Proceedings of the IEEE*, 2010.

[18] C. Stillinger, T. K. A. Brekken, A. von Jouanne, R. Paasch, D. Naviaux, K. Rhinefrank, J. Prudell, A. Schacher, and E. Hammagren, "WEC prototype advancement with consideration of a real- time damage accumulation algorithm," in *PowerTech*, Trondheim, Norway, 2011.

[19] E. Amon, A. Schacher, and T. K. A. Brekken, *A maximum power point tracking algorithm for ocean wave energy devices*, IEEE Ind. Application Magazine to be published.

[20] E. Amon, A. Schacher, and T. Brekken, "A novel maximum power point tracking algorithm for ocean wave energy devices," in *Energy Conversion Congr. and Exposition (ECCE)*, 2009, pp. 2635–2641.

[21] A. Bensoussan, D. P. Giuseppe, M. C. Delfour, and S. K. Mitter, *Representation and Control of Infinite Dimensional Systems*, 2nd ed. Springer, 2007.

[22] J. A. Atwell and B. B. King, "Proper orthogonal decomposition for reduced basis feedback controllers for parabolic equations," *Mathematical and Computer Modeling*, no. 33, pp. 1–19, 2001.

[23] B. Moore, "Principal component analysis in linear systems: Controllability, observability, and model reduction," *Automatic Control, IEEE Transactions on*, vol. 26, no. 1, pp. 17–32, Feb 1981.

[24] K. A. Evans, "Reduced order controllers for distributed parameter systems," Ph.D. dissertation, Virginia Polytechnic Institute and State University, 2003.

[25] C. Lee and H. Tran, "Reduced-order-based feedback control of the kuramoto–sivashinsky equation," *Journal of Computational and Applied Mathematics*, vol. 173, no. 1, pp. 1 – 19, 2005. [Online]. Available: http://www.sciencedirect.com/science/article/pii/S0377042704001268

[26] S. Tan and L. He, *Advanced Model Order Reduction Techniques in VLSI Design*. Cambridge University Press, 2007.

[27] E. E. Vidal-Rosas, S. A. Billings, Y. Zheng, J. E. Mayhew, D. Johnston, A. J. Kennerley, and D. Coca, "Reduced-order modeling of light transport in tissue for real-time monitoring of brain hemodynamics using diffuse optical tomography," *Journal of biomedical optics*, 2014.

[28] S. S. Swei, G. G. Zhu, and N. T. Nguyen, "Integrated model reduction and control of aircraft with flexible wings," in *AIAA Guidance, Navigation, and Control (GNC) Conference*, 2013.

[29] K. A. Smith, C. D. Rahn, and C. Wang, "Model order reduction of 1D diffusion systems via residue grouping," *Journal of Dynamic Systems, Measurement, and Control*, vol. 130, 2008.

[30] A. C. Antoulas, D. C. Sorensen, and S. Gugercin, "A survey of model reduction methods for large-scale systems," *Contemporary Mathematics*, vol. 280, pp. 193–219, 2001.

[31] J. L. Lumley, "Stochastic tools in turbulence," *Journal of Fluid Mechanics*, vol. 67, no. 413-415, 1975.

[32] L. Sirovich, "Turbulence and the dynamics of coherent structures. i - coherent structures. ii - symmetries and transformations. iii - dynamics and scaling," *Quarterly of Applied Mathematics*, vol. 45, pp. 561–571, 573–590., 1987.

[33] N. Aubry, P. Holmes, J. L. Lumley, and E. Stone, "The dynamics of coherent structures in the wall region of a turbulent boundary layer," *Journal of Fluid Mechanics*, vol. 192, pp. 115–173, 1988.

[34] P. Holmes, J. L. Lumley, and G. Berkooz, *Turbulence, Coherent Structures, Dynamical Systems and Symmetry*. Cambridge University Press, 1996.

[35] S. S. Ravindran, "A reduced-order approach for optimal control of fluids using proper orthogonal decomposition," *International Journal for Numerical Methods in Fluids*, vol. 34, no. 5, pp. 425–448, 2000. [Online]. Available: http://dx.doi.org/10.1002/1097-0363(20001115)34:5⟨425::AID-FLD67⟩3.0.CO;2-W

[36] M. Couplet, C. Basdevant, and P. Sagaut, "Calibrated reduced-order pod-galerkin system for fluid flow modeling," *Journal of Computational Physics*, pp. 192–220, 2005.

[37] B. Galletti, C. Bruneau, L. Zannetti, and A. Iollo, "Low-order modeling of laminar flow regimes past a confined square cylinder," *Journal of Fluid Mechanics*, vol. 503, pp. 161–170, 2004.

[38] P. J. Holmes, J. L. Lumley, G. Berkooz, J. C. Mattingly, and R. W. Wittenberg, "Low-dimensional models of coherent structures in turbulence," *Physics Reports*, vol. 287, no. 4, pp. 337 – 384, 1997. [Online]. Available: http://www.sciencedirect.com/science/article/pii/S0370157397000173

[39] W. K. Pratt, *Digital image processing*, 2nd ed. Wiley, 1991.

[40] C. W. Rowley and B. A. Batten, *Dynamic and closed-loop control*. Chapter 5 in Fundamentals and Applications of Modern Flow Control, R. D. Joslin and D. N. Miller, Editors, AIAA Progress in Astronautics and Aeronautics, 2009.

[41] R. Everson and L. Sirovich, "Karhunen-Loève procedure for gappy data," *Journal of the Optical Society of America A: Optics, Image Science, and Vision*, vol. 12, pp. 1657–1664, 1995.

[42] C. W. Rowley and J. E. Marsden, "Reconstruction equations and the Karhunen–Loève expansion for systems with symmetry," *Physica D: Nonlinear Phenomena*, vol. 142, no. 1–2, pp. 1 – 19, 2000. [Online]. Available: http://www.sciencedirect.com/science/article/pii/S0167278900000427

[43] D. G. Aronson, S. I. Betelu, and I. G. Kevrekidis, "Going with the flow: a Lagrangian approach to self-similar dynamics and its consequences," 2001.

[44] C. W. Rowley, I. G. Kevrekidis, J. E. Marsden, and K. Lust, "Reduction and reconstruction for self-similar dynamical systems," *Nonlinearity*, vol. 16, pp. 1257–1275, 2003.

[45] W. Beyn and V. Thümmler, "Freezing solutions of equivariant evolution equations," *SIAM Journal on Applied Dynamical Systems*, vol. 3, no. 2, pp. 85–116, 2004. [Online]. Available: http://dx.doi.org/10.1137/030600515

[46] B. Noack, K. Afanasiev, M. Morzyński, G. Tadmor, and F. Thiele, "A hierarchy of low-dimensional models for the transient and post-transient cylinder wake," *Journal of Fluid Mechanics*, vol. 497, pp. 335–363, 2003.

[47] G. E. Dullerud and F. Paganini, *A Course in Robust Control Theory: A Convex Approach*. Springer-Verlag, 1999.

[48] B. N. Datta, *Numerical Methods for Linear Control Systems*. Elsevier, 2004.

[49] S. Lall and J. E. Marsden, "A subspace approach to balanced truncation for model reduction of nonlinear control systems," *International Journal on Robust and Nonlinear Control*, vol. 12, pp. 519–535, 2002.

[50] M. Ilak and C. W. Rowley, "Modeling of transitional channel flow using balanced proper orthogonal decomposition," *Physics of Fluids (1994-present)*, vol. 20, no. 3, pp. –, 2008. [Online]. Available: http://scitation.aip.org/content/aip/journal/pof2/20/3/10.1063/1.2840197

[51] J. R. Singler and B. A. Batten, "Balanced proper orthogonal decomposition for model reduction of infinite dimensional linear systems," in *Proceedings of the International Conference on Computational and Mathematical Methods in Science and Engineering, CMMSE*, 2007.

[52] J. Singler and B. A. Batten, "A proper orthogonal decomposition approach to approximate balanced truncation of infinite dimensional linear systems," *Int. J. Comput. Math.*, vol. 86, no. 2, pp. 355–371, Feb. 2009.

[53] R. F. Curtain and H. J. Zwart, *An Introduction to Infinite-Dimensional Linear System Theory*. Springer-Verlag, 1995.

[54] J. R. Singler and B. A. Batten, "Model reduction of a heuristic 1D PDE model for a wave energy converter in a wave tank," in *Preparation*.

[55] P. Dorato, C. Abdallah, and V. Cerone, *Linear Quadratic Control: An Introduction*. Prentice Hall PTR, 1995.

[56] M. Tucker and E. Pitt, *Waves in Ocean Engineering*. Elsevier, 2001.

[57] J. F. chot, "Realistic simulation of ocean surface using wave spectra," *Journal of Virtual Reality and Broadcasting*, vol. 4, no. 11, 2007.